Durability-Enhanced VO_2 Thermochromic Film for Smart Windows

Xinpeng Zhao[2,#], Sohrab A. Mofid[2,3,#], Tao Gao[3], Gang Tan[4], Bjørn Petter Jelle[3,5,*], Xiaobo Yin[2,*], and Ronggui Yang[1,*]

[1]School of Energy and Power Engineering, Huazhong University of Science and Technology, Wuhan, Hubei 430074, China.

[2]Department of Mechanical Engineering, University of Colorado, Boulder, Colorado 80309, USA.

[3]Department of Civil and Environmental Engineering, Norwegian University of Science and Technology (NTNU), NO-7491 Trondheim, Norway.

[4] Department of Civil and Architectural Engineering, University of Wyoming, Laramie, Wyoming 82071, USA.

[5]Department of Materials and Structures, SINTEF Community, NO-7465 Trondheim, Norway.

# These authors contribute equally.

*E-mail: ronggui@hust.edu.cn

xiaobo.yin@colorado.edu

bjorn.petter.jelle@ntnu.no

Abstract

Vanadium dioxide (VO_2) based thermochromic films are of great interest for energy-saving smart windows as they can dynamically change the solar transmittance as the ambient temperature changes. However, VO_2 is thermodynamically unstable and could be easily oxidized by the oxygen and moisture in the ambient air. In this work, a durability-enhanced VO_2 nanoparticle-polymer thermochromic film was proposed and fabricated using the blade coating method where the cross-linked and highly entangled poly (methyl methacrylate) (PMMA) chain with molecular weight (~

950,000) was adopted to block gas diffusion in the polymer matrix. It was shown that the developed VO_2 nanoparticles film kept ~ 30% of the solar modulation ability after ~ 900 hours of accelerated durability test in the aging environment with a temperature at 60 ºC and ~ 95% humidity. This is ~ 4 times of the lifetime of the VO_2 nanoparticles which are embedded in the non-cross-linked PMMA matrix with low molecular weight (~ 15,000). The cross-linked PMMA-VO_2 film also showed a high luminous transmittance of ~ 50%, a high solar modulation ability of ~17% and a low haze of ~ 11%. Our method provides an easy and effective strategy to improve the lifetime of VO_2 nanoparticles, showing a promising pathway toward environmentally stable and easily scalable thermochromic films for energy-efficient smart windows.

Keywords: Vanadium dioxide nanoparticle, Cross-linking, Thermochromic, Smart window.

I. Introduction

With a high solar transmittance > 90%, as much as ~ 800 W/m^2 solar irradiation reaches the indoor environment through windows during daytime [1, 2]. The transmitted solar energy greatly reduces the energy consumption for heating in cold climates. However, excessive solar heating would result in increased cooling loads in hot climates, especially in summer. Smart windows that could dynamically adjust the transmittance of solar irradiation have been thought of as one of the most promising techniques to reduce the energy consumption of buildings [3, 4]. In particular, there are a lot of interests in vanadium dioxide (VO_2) nanoparticle and transparent polymer matrix based thermochromic films in recent years, especially due to the relatively high luminous transmittance of ~ 50%, and solar modulation ability of ~ 20% [5-11]. However, pristine VO_2 is thermodynamically unstable and can be easily oxidized to V_2O_5 when exposed to air for several months [12, 13], which in turn dramatically reduces the solar modulation ability. A humid environment would also greatly accelerate the oxidation process. Previous studies [8, 14-16]

showed that the thermochromic performance of VO_2 decreased noticeably when exposed to relatively high humidity for only ~ 24 hours, deterring the practical deployment of VO_2 based smart windows.

To improve the anti-oxidation ability and increase the lifetime of VO_2 nanoparticles, core-shell nanoparticles have been proposed, where the environmentally stable materials are used as a protection layer to prevent VO_2 from water and oxygen exposure and hence to decrease the oxidation rate. For example, the previous study showed that employing aluminum oxide based shells could increase the lifetime of VO_2 from ~ 3 days to more than ~ 20 days under accelerated aging tests with a 60 ºC temperature and 90% relative humidity[16]. In addition, other environmentally stable oxides like SiO_2 [10], TiO_2 [17], and ZnO [8] have been used to increase the durability of VO_2 nanoparticles. However, in practical applications, when VO_2 nanoparticles transit periodically from monoclinic (M, $a_M = 5.75, b_M = 4.52$ Å, $c_M = 5.38$ Å, $\beta = 122.6°$) structure to tetragonal rutile (R, $a_R = b_R = 4.55$ Å, $c_R = 2.86$ Å) structure [6], the interface stress between the VO_2 cores and oxide protection shells induced by the lattice structure transformation of VO_2 nanoparticles may result in the formation of micro cracks at the interface. A recent study [18] has shown that cracks occur in VO_2 based multilayer thin films after ~ 1000 times of reversible phase transitions. In addition, cracks were even found in SiO_2 [19] and TiO_2 shells [8, 17] during the synthesis process. The accelerated aging tests at a temperature of 60 ºC and 90% relative humidity showed that the lifetime of the SiO_2 coated VO_2 nanoparticles were only ~ 72 hours due to the appearance of such cracks [8]. It is also worthwhile to note that although the introduction of a shell layer potentially enhances the durability of VO_2 nanoparticles and improves the solar luminous transmittance, it may lower the solar modulation ability of the film. For example, the experimental results by Li *et al.* showed that the solar modulation ability decreased ~ 50% when

the VO_2 nanoparticles were coated by ~ 7 nm thick TiO_2 shells [17]. Besides the core-shell nanoparticle structures, blocking the diffusion of oxygen and moisture in the polymer matrix may also delay the oxidation process of VO_2 nanoparticles. In general, increasing the molecular weight (length) of polymer chain and generating chemical crosslinks between neighboring polymer chains are two effective ways to reduce gas diffusion in polymer matrix because the mobility of polymer chains can be restricted by the highly entangled polymer chains and the ionic or covalent bonds between neighboring polymer chains [20-24]. A previous study by Berens *et al.* showed that the diffusivity of organic vapors (e.g., $(CH_3)_2CO$, $CHCl_3$) was decreased by a factor of ~ 10 when the molecular weight of polystyrene increased from 10,000 to 300,000 [25]. Klinger *et al.* showed that a 0.45% mole percentage of cross-linking in poly(methyl methacrylate) (PMMA) could reduce the oxygen diffusion coefficient by ~ 30% [26]. These together imply that highly cross-linked high molecular weight polymers may provide a simple and yet effective pathway to protect the randomly dispersed VO_2 nanoparticles from oxidation.

Considering the high transparency, structural stability, and easy to crosslink, a cross-linked high molecular weight PMMA film (~ 950,000) embedded with VO_2 nanoparticles with a size of 50 ~ 80 nm was demonstrated in this work. The developed PMMA-VO_2 film with a thickness of ~ 4 μm has a relatively high luminous transmittance of ~ 50%, solar modulation ability of ~17.1%, and a low haze value of ~ 11%. The accelerated aging test at a temperature of 60 ºC and a relative humidity of ~ 95% showed that the lifetime of the VO_2 nanoparticles dispersed in the cross-linked high molecular weight PMMA film (~ 950,000) is more than 900 hours, which is much longer than that of VO_2 nanoparticles in the non-cross-linked low molecular weight (~ 15,000) PMMA, around 200 hours. The lifetime of VO_2 nanoparticles in the cross-linked and entangled PMMA matrix is significantly longer than the reported VO_2 nanoparticles coated by SiO_2 (~ 72 hours) ,

$Al(OH)_3$ (~ 120 hours) , and VO_2 thin film protected by Al_2O_3 (~ 100 hours) [14], and is comparable to the VO_2 nanoparticles coated by Al_2O_3 (> 480 hours) [16], and VO_2 thin film protected by SiN_x (~ 600 hours) [18]. The fatigue test shows that the thermochromic performance of the developed PMMA-VO_2 films keeps the same after 3000 times of continuous reversible phase transitions. The analysis also shows that the developed PMMA-VO_2 film could greatly reduce the cooling demands in hot climates and improve the thermal comfort and condensation resistance in cold climates.

II. Materials and methods

2.1 Synthesis

2.1.1 Chemicals and materials

Vanadium pentoxide (V_2O_5, 99.99%, Sigma Aldrich), oxalic acid dihydrate ($H_2C_2O_4 \cdot 2H_2O$, 99%, Sigma Aldrich), poly (methyl methacrylate) (PMMA, molecular weight ~15,000 (15K), Sigma Aldrich), and anisole (C_7H_8O, 99.7%, Sigma Aldrich), PMMA A4 (molecular weight ~950,000 (950K), MicroChem Corp) resists in anisole were purchased and used as as-supplied without additional purifications.

2.1.2 Synthesis of monoclinic *VO_2 (M)*

Various synthesis methods of monoclinic VO_2 (M) could be found in the earlier studies [8, 10, 27-29]. In this work, VO_2 nanoparticles were synthesized by the hydrothermal method [8]. For a typical synthesis, 2.0 g of V_2O_5 powder was added to 40.0 ml deionized water and was stirred for 20 min, then 3.4 g of oxalic acid dihydrate was added to the mixture and further stirred until a clear light green/blue slurry was formed. The suspension was then moved to a 150 ml Teflon-lined stainless-steel autoclave. The autoclave was kept at 260 °C for 24.0 h and then air-cooled to room

temperature. The resulting black-precipitates was collected and washed with deionized water and ethanol 3 times, respectively, then dried with a vacuum furnace at 120 °C for 5.0 h. A schematic illustrating the synthesis process could be found in Fig. 1(a).

2.2 Measurements

The commercial Netzsch differential scanning calorimetry (DSC 204 F1 Phoenix) was used to determine the phase transition properties of the synthesized VO_2 powder over the temperature range from 0 to 100 °C, and the heat absorption properties of the PMMAs from 0 to 550 °C, respectively. The heating/cooling rate was set at 10 °C/min. The crystalline phase of the VO_2 powder was identified using X-ray diffraction (XRD, MiniFlex600, Rigaku, Japan) with Cu Kα radiation (λ = 1.5418) at a voltage 40 kV and a current of 40 mA. Transmission electron microscope (TEM, JEM-2010) was used to characterize the morphology and microstructure of the nanoparticles. Optical performance, including spectral transmittance and haze of the films, was measured using a UV-Vis-Near-IR spectrophotometer (Shimadzu UV-3101) together with a temperature control unit including black anodized aluminum 6061 plate, and a variac (2 A, 120 V). A helium-neon (HeNe) laser (SIEMENS), and a programmable stage temperature controller (LINKAM TMS 94) together with a heating/freezing microscope stage (LINKAM MDS600) with a microscope objective lens (NIKON, Plan Fluor ELWD 20x/0.45) was assembled to measure the reflectance spectrum of the film with a 200 nm silver coating in 633 nm at 25 °C and 90 °C with ramping rate 10 °C/min. A TPS (TENNEY) environmental chamber was used to create a steady-state temperature and humidity (60 °C, relative humidity ~ 95%) for the durability testing of the PMMA-VO_2 films.

III. Results and discussion

3.1 Fabrication and characterization of PMMA-VO_2 film

PMMA is a non-toxic, inexpensive thermoplastic with high optical transparency, high mechanical strength and durability, excellent thermal stability, and weather resistance [30]. PMMA with different molecular weights (chain length and entanglement) could be obtained and processed easily [31]. Moreover, the influence of the near-UV from solar radiation on the PMMA is minor since PMMA is only sensitive to high energy radiation such as the electron beam, x-rays, and UV radiation with wavelengths shorter than 300 nm [31, 32]. Thus, PMMA was adopted as the polymer matrix in this work. As shown in Fig. 1(b), the desired amount of as-synthesized crystalline monoclinic VO_2 nanoparticles was dispersed ultrasonically into 40 ml of PMMA 950K A4. The solution was then stirred at room temperature for 12 hours. Generally, the molecule chains of PMMA could be interlinked using several methods, including free radical polymerization, condensation reactions, small molecule crosslinking, and radiation [33]. Wochnowski *et al*. showed that the 248nm-wavelength ultraviolet (UV) irradiation could crosslink the two neighboring PMMA molecules by establishing an oxygen bridge between *ester* side chains or connecting the two *carbonyl* groups [32]. The degree of crosslinking of the PMMA matrix could be controlled by both the dose and the duration of the UV irradiation. A higher degree of crosslinking usually has a higher endothermic peak, which can be evaluated by the DSC measurements. The radiation dose needs to be smaller than 2.0 J/cm^2 to prevent the brittleness of PMMA film after crosslinking [34]. Here the PMMA/VO_2 solution was irradiated by the UV radiation (220 ~380 nm, ADJ Products) for 10 hours in the room environment while being stirred at 300 rpm to generate crosslinks in the PMMA matrix. The final mixture was maintained at a constant temperature of ~ 75 °C on a hotplate for 40 min. The solution was then loaded onto a ~ 50 μm thick transparent and chemically stable biaxially-oriented polyethylene terephthalate (BoPET) sheet laminated on a piece of float glass using blade coating method as shown in Fig.

1(b). The final thickness of the dried PMMA-VO_2 film is determined by the concentration of PMMA, the moving speed of the blade, and the gap between the blade tip and the substrate. Here the film was formed using blade coating at a speed of 15mm/s. After the wet film is fabricated, the film is dried in a fume hood for 2 hours. Finally, a thin film with an area of 600 mm × 300 mm (length × width) and a thickness of ~ 4 μm is obtained as shown in Fig. 1(c), in which the PMMA-VO_2 film is coated on a 50 μm thick BoPET film. No obvious variation of the film brittleness was observed.

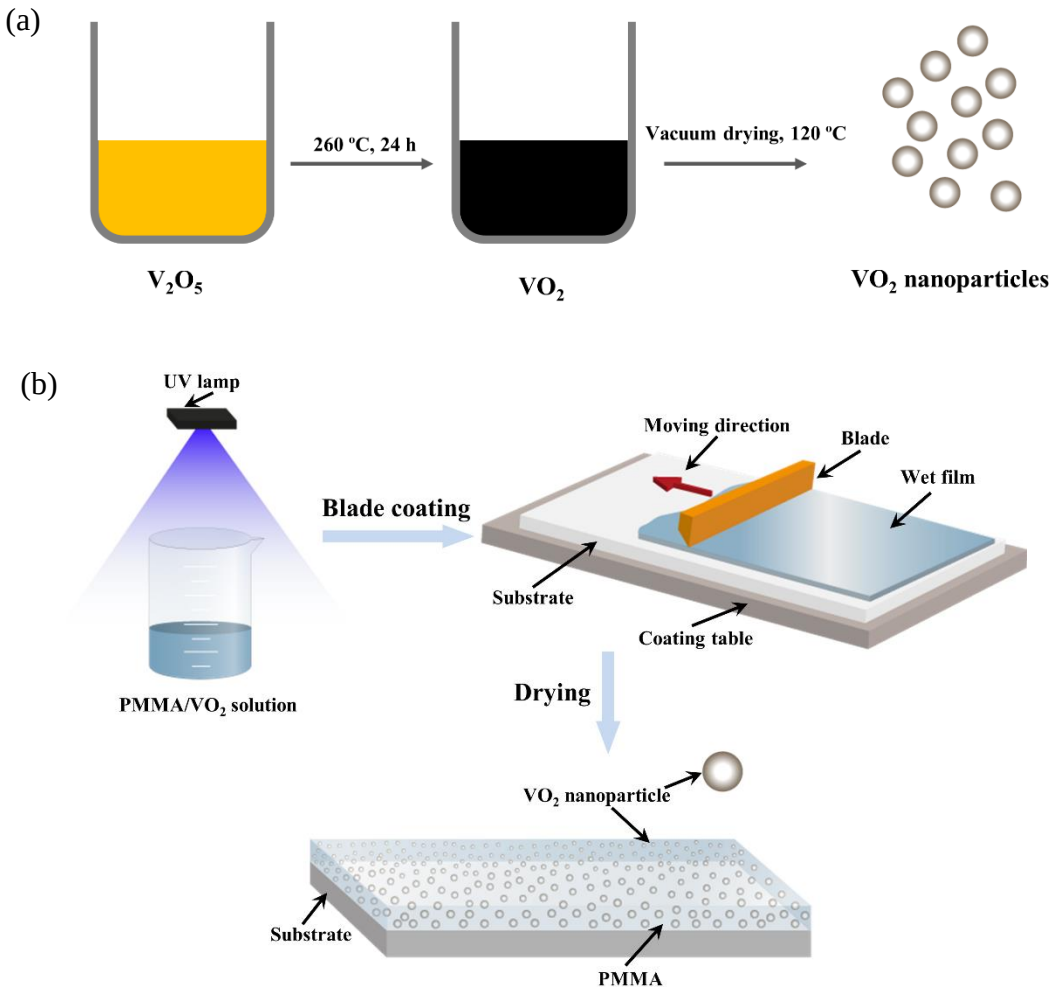

(c) 

Figure 1. Fabrication of durability-enhanced PMMA-VO_2 thermochromic film for smart windows. (a) Synthesis process of VO_2 nanoparticles using the hydrothermal method. (b) Schematic of the fabrication process of the meter-scale durability-enhanced PMMA-VO_2 film using the blade coating method. The PMMA/VO_2 solution was first exposed to ultraviolet (UV) rays. Then, the wet PMMA-VO_2 film was fabricated using the blade coating method. After drying, the PMMA-VO_2 composite film was obtained. (c) Snapshot of a PMMA-VO_2 film with a size of 600 mm × 300 mm (length × width) manufactured using the blade coating method, in which a ~ 4.0 μm thick PMMA-VO_2 film is coated on a 50 μm thick BoPET film.

Figure 2(a) shows the morphology of VO_2 nanoparticles from transmission electron microscopy (TEM). It is seen that most of the nanoparticles have an approximately spherical shape, and the diameter of the VO_2 nanoparticles mainly lies in the range of 50 ~ 80 nm. Fig. 2(b) presents the X-Ray Diffraction (XRD) measurement of the VO_2 nanoparticles, where the diffraction peaks indicate that the VO_2 nanoparticles are in the monoclinic phase (M2, C2/m) [12]. The phase transition temperature of the VO_2 nanoparticles was determined by differential scanning calorimetry (DSC) measurements using a heating/cooling rate of 10 ºC/min in the temperature

range from 0 to 110 °C. Since the insulator-to-metal transformation of VO_2 is a first-order phase transition [35], the discontinuous variation of entropy results in the release or absorption of latent heat. As shown in Fig. 2 (c), when VO_2 transits from the monoclinic (M) insulator phase to the rutile (R) phase during the heating cycle, an endothermic (positive) peak with peak temperature ~ 71 °C is observed. A corresponding exothermic (negative) peak, representing metal-to-insulator transition, occurs in the cooling cycle, where the peak temperature is ~ 63 ºC. This DSC curve is similar to those reported in the literature [8, 11, 36]. Since the crosslinking process could generate new chemical bonding between neighboring chains, the cross-linked PMMA polymers are expected to have a higher endothermic peak and a larger maximum decomposition temperature [37]. Figure 2(d) compares the DSC thermographs of cross-linked PMMA and non-cross-linked PMMA with molecular weight ~ 950,000. Comparing to the non-UV exposed 950,000 PMMA, the 950,000 PMMA under UV exposure has a higher endothermic peak (from ~ 6.0 μV/mg to ~ 9.5 μV/mg) and a larger maximum decomposition temperature (from 375 ºC to 386 ºC), indicating the crosslinks were generated.

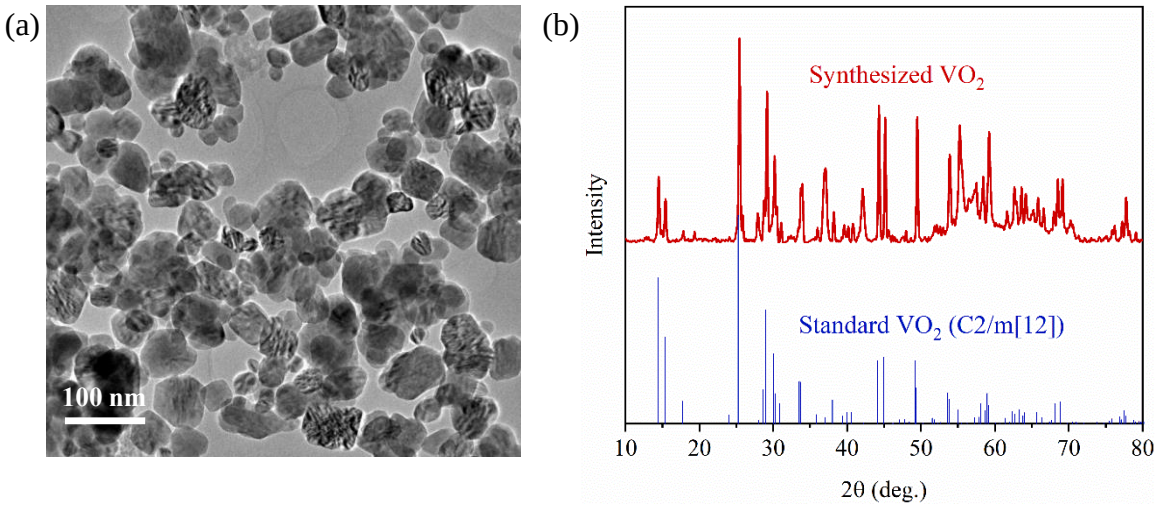

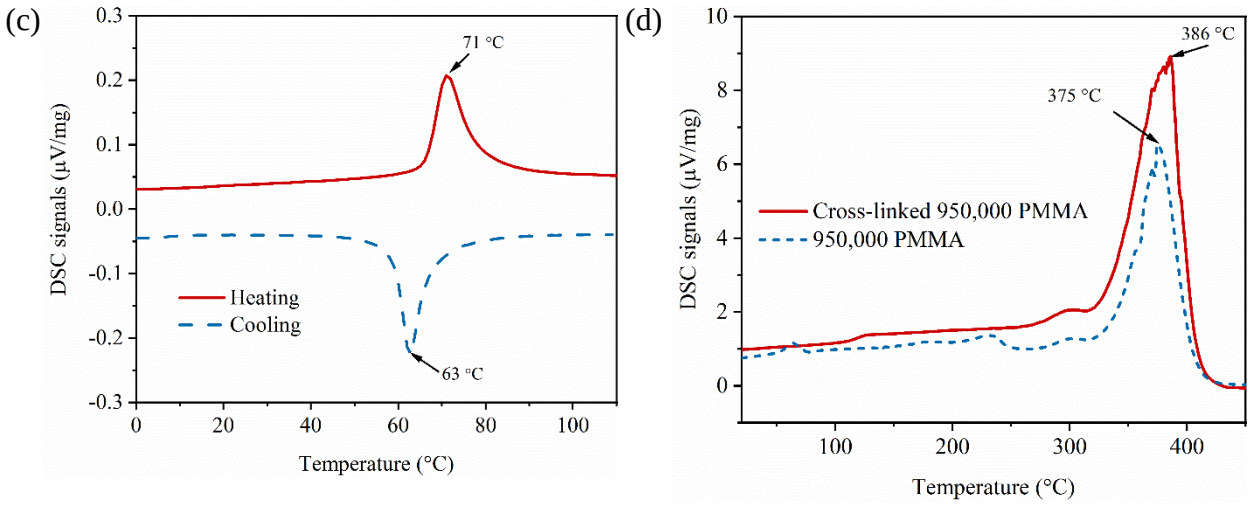

Figure 2. Characterization of the synthesized VO_2 nanoparticles. (a) Transmission electron microscopy (TEM) image of the VO_2 nanoparticles. (b) X-Ray Diffraction (XRD) pattern of the VO_2 nanoparticles. (c) Differential scanning calorimetry (DSC) of the VO_2 nanoparticles, where the heating/cooling rate is set at 10 ºC/min. (d) Comparison of the DSC thermograms of the cross-linked and non-cross-linked PMMA with molecular weight ~ 950,000. The positive peak represents an endothermic process, and the negative peak represents an exothermic process.

3.2 Optical performances of PMMA-VO_2 film

To evaluate the thermochromic performance of the PMMA-VO_2 film, the total transmittance and haze, were both measured using a commercial UV-Vis-Near-IR spectrophotometer (Shimadzu UV-3101). The total transmittance ($\tau_{\lambda,tot}$) were measured by placing the PMMA-VO_2 film and a diffuse reflector at the inlet and outlet of the integrating sphere, respectively. The measured total spectral transmittances of the PMMA-VO_2 film at low temperature (~ 25 ºC) and high temperature (~ 90 °C) are shown in Fig. 3(a). Since the metallic phase VO_2 blocks the near-infrared (NIR) solar radiation, it was found that the transmittance of the PMMA-VO_2 in the range of 800 ~ 2500 nm was much smaller when the temperature of the

PMMA-VO_2 film was set at ~ 90 ºC. The mean luminous (380-780 nm) transmittance τ_{lum} and mean solar (280-2500 nm) transmittance τ_{sol} were then calculated as,

$$\tau_{lum} = \frac{\int_{380\ nm}^{780\ nm} I_{lum,\lambda}\tau_{\lambda,tot}d\lambda}{\int_{380\ nm}^{780\ nm} I_{lum,\lambda}d\lambda} \quad (1)$$

$$\tau_{sol} = \frac{\int_{280\ nm}^{2500\ nm} I_{sol,\lambda}\tau_{\lambda,tot}d\lambda}{\int_{280\ nm}^{2500\ nm} I_{sol,\lambda}d\lambda} \quad (2)$$

where $I_{lum,\lambda}$ is the standard luminous efficiency function for vision [38], $I_{sol,\lambda}$ is the solar radiation intensity of air mass 1.5 (AM1.5) corresponding to the sun standing 37° above the horizon [39], and $\tau_{\lambda,tot}$ is the total transmittance of radiation at wavelength λ shown in Fig. 3(a). The solar modulation ability $\Delta\tau_{sol}$ is defined by the difference of solar transmittance before and after the phase transition, *i.e.*,

$$\Delta\tau_{sol} = \tau_{sol}(T < T_c) - \tau_{sol}(T > T_c) \quad (3)$$

where T_r is the critical phase change temperature of VO_2. According to Eqs. (1-2), the luminous transmittance at low temperature and solar modulation ability are calculated to be ~ 50% and ~17.1%, respectively. Besides, we have also checked the uniformity of the coating by measuring the transmittance of the film at several different locations. The difference of the solar transmittances among different points was found to be smaller than 1%.

Haze is used to characterize the percentage of the transmitted light whose propagation direction deviates a specific angle from the direction of the incident beam. According to the ASTM D1003-13 [40], haze is defined as,

$$H_\lambda = \frac{\tau_{dif,\lambda}}{\tau_{tot,\lambda}} = \frac{\tau_{dif,\lambda}}{\tau_{dif,\lambda} + \tau_{dir,\lambda}} \quad (4)$$

where $\tau_{dif,\lambda}$ refers to the light scattered more than 2.5° off from the incident light [40], and $\tau_{dir,\lambda}$ is the transmitted light within the angle of 2.5°. The diffuse transmittance can be measured by replacing the diffuse reflector at the outlet of the integrating sphere with a light trap to prevent the direct transmittance from influencing the measurement signal. Since the VO_2 nanoparticle size (50 to 80 nm) is much smaller than the wavelength of the visible light (400~ 800 nm), the scattering of the light passing through the PMMA-VO_2 films can be described by Rayleigh scattering [41]. Therefore, it is seen that the haze value decreases as the wavelength increase in Fig. 3(b). The averaged haze value in the visible range is calculated as,

$$H = \frac{\int_{380\ nm}^{780\ nm} H_\lambda I_{lum,\lambda} d\lambda}{\int_{380\ nm}^{780\ nm} I_{lum,\lambda} d\lambda} \tag{5}$$

where H_λ is the measured haze value at wavelength λ. According to Eq. (5), the averaged haze in the luminous range is ~ 11%, as shown in Fig. 3(b). Note that the haze of the developed film could be lowered by reducing the size of the VO_2 nanoparticles [41]. In short, we have fabricated a large-size PMMA-VO_2 film with high luminous transmittance (~ 50%), large solar modulation ability (~ 17.1%), and relatively low haze visibly (~ 11%).

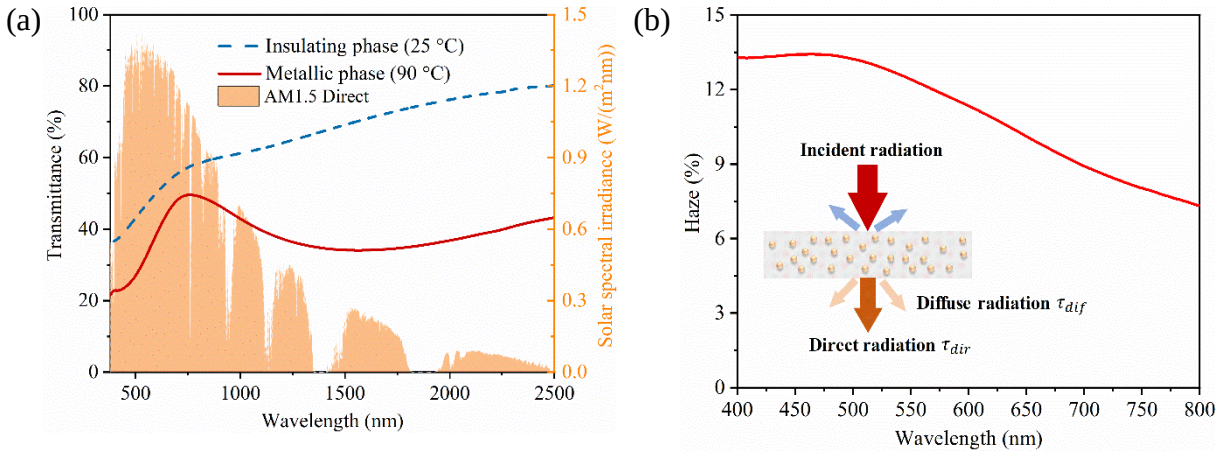

Figure 3. The optical performance of the PMMA-VO_2 film. (a) Spectral transmittance of the PMMA-VO_2 film in the solar spectrum, where the luminous transmittance is ~ 50% and the solar modulation ability is ~ 17.1%. (b) The spectral haze of the PMMA-VO_2 film in the visible range with wavelengths of 400 ~ 800 nm, the averaged haze is ~ 11%.

3.3 Durability of PMMA-VO_2 film

Oxygen and moisture in the ambient air could diffuse into the polymer matrix and oxidize the phase-switchable VO_2 to non-switchable V_2O_5, resulting in the loss of solar modulation ability. It is thus desirable to reduce the diffusion capacity of gas molecules in the polymer matrix. The previous studies have shown that the thermal stability [37], surface hardness, and chemical resistance [42] of the polymer matrix could be improved significantly using entangled and cross-linked molecular chains, which is also directly related to a smaller gas diffusion coefficient. In practice, the natural oxidation of VO_2 is a long process, and the obvious variation of the thermochromic property in the ambient conditions may only be observed after a few months [12]. Thus, accelerated environmental tests were performed to evaluate the durability of VO_2 nanoparticles [43, 44]. The tests were conducted at a temperature of 60 ºC, and the relative humidity ~ 95%, similar to the testing conditions reported in the previous studies [8, 18].

Systematic measurements of spectral transmittance at both low temperature (25 ºC, insulating phase) and high temperature (90 °C, metallic phase) were recorded as a function of time to determine the variation of the thermochromic performance. Each measurement was then repeated at least three times to ensure the testing reliability. To investigate the influence of crosslinking and entanglement on the durability of the PMMA-VO_2 film, the cross-linked and non-crossed-linked PMMA-VO_2 film with two different molecular weights were measured. It is seen that the cross-linked PMMA film with molecular weight ~ 950,000 exhibits no noticeable change in optical transmittance after ~ 200 hours, as shown in Fig. 4 (a). The thermochromic properties of cross-linked PMMA-VO_2 film with molecular weight ~ 950,000 begin to deteriorate after ~ 450 hours exposure while still maintaining more than 60% of its solar modulation ability (~ 10%). After about ~ 900 hours, the solar modulation ability decreased from ~ 17.1% to ~ 4.0%, indicating that a large part of the VO_2 nanoparticles was oxidized. For comparison, the durability performances of the non-cross-linked PMMA with molecular weights ~ 15,000 (Fig. 4(b)) and ~ 950,000 (Fig. 4(c)) were also tested under the same accelerated testing conditions (60 ºC, humidity > 95%). Fig. 4(d) gives the variation of solar modulation abilities of the above three PMMA-VO_2 films as a function of time. It is seen that the decreasing rate of the non-cross-linked film with molecular weight ~ 15,000 is much faster than that of the non-cross-linked PMMA with molecular weight ~ 950,000, which is close to decreasing rate of the uncoated VO_2 in the matrix of resin[16]. The thermochromic performance of the VO_2 in the non-cross-linked PMMA with molecular weights ~ 15,000 disappears after ~ 200 hours. Furthermore, it is found that the lifetime of the cross-linked 950,000 PMMA was approximately 350 hours longer than of non-cross-linked 950,000 PMMA at ~ 600 hours. This indicates that the entangled and crosslinked polymer matrix can substantially improve the lifetime of VO_2 nanoparticles. Fig. 4(d) shows that the lifetime of the PMMA-VO_2

film developed in this work is better than the previously reported values for VO_2 nanoparticles coated by SiO_2 (~ 72 hours) [8], $Al(OH)_3$ (~ 120 hours) [8], and VO_2 thin film protected by Al_2O_3 (~ 100 hours) [14], and is comparable to the performances of VO_2 nanoparticles coated by Al_2O_3 (> 480 hours) [16] and VO_2 thin film protected by SiN_x (~ 600 hours) [18]. Clearly we have demonstrated here an alternative pathway to effectively improve the lifetime of the VO_2 nanoparticles, avoiding the emergence of cracks induced by the periodic insulator-to-metal phase change found in the core-shell structures.

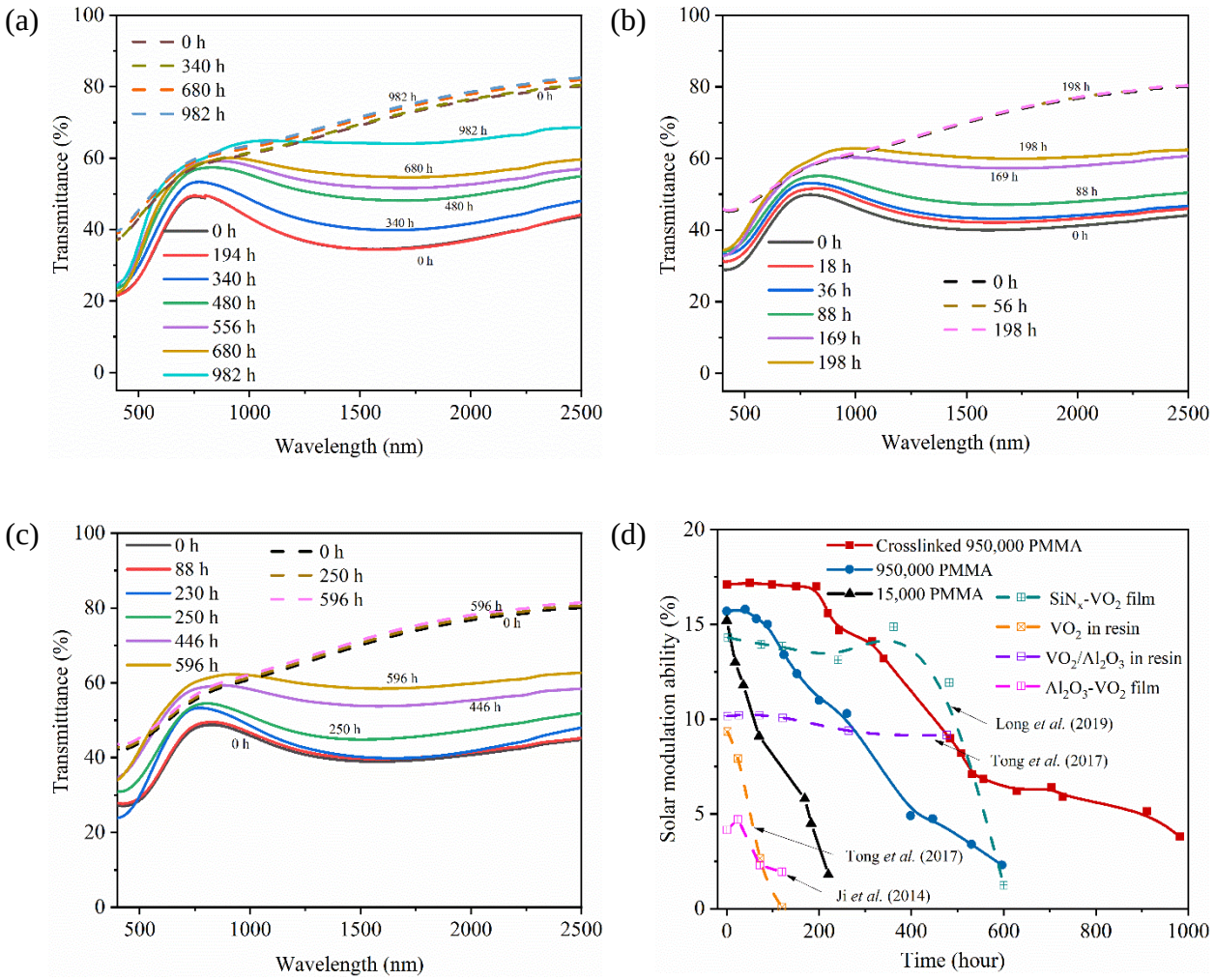

Figure 4. Durability performance of the PMMA-VO_2 films. (a) Variation of the spectral optical transmittance of VO_2 nanoparticles embedded in cross-linked 950,000 PMMA matrix as a function

of aging time. (b) Variation of the spectral optical transmittance of VO_2 nanoparticles embedded in the non-cross-linked 150,000 PMMA matrix as a function of aging time. (c) Variation of the spectral optical transmittance of VO_2 nanoparticles embedded in the non-cross-linked 950,000 PMMA matrix as a function of aging time. (d) Comparison of the solar modulation ability of the VO_2 nanoparticles embedded in non-cross-linked 150,000 PMMA, non-cross-linked 950,000 PMMA, cross-linked 950,000 PMMA matrixes, and previous studies [14, 16, 18]. The low and high temperatures for the optical measurements are 25 ºC (insulating phase) and 90 ºC (metallic phase), respectively. The aging tests were performed in the accelerated aging chamber with a temperature at 60 ºC, and the relative humidity is ~ 95%.

Fatigue tests are used to determine the numbers of cycles (fatigue life) that a material or structure can withstand under cyclic loadings. The emergence of cracks in VO_2-based films or complete fractures may occur due to the lattice transformation of VO_2 during many cycles of phase transitions from the insulating to the metallic state. Therefore, the fatigue test is performed to study the stability of the developed PMMA-VO_2 thermochromic film. The design of the fatigue test can be seen in Fig. 5(a). The PMMA-VO_2 sample coated with a ~ 100 nm thick bottom silver layer was placed on a programmable stage with a temperature control unit (LINKAM MDS600), where the ramping rate was set at (10 °C/min) and an extra 45 seconds delay was assigned to stabilize the temperature of the film at both 25 °C and 90 °C. Meanwhile, the film was constantly exposed to a 633 nm focused laser beam from the helium-neon (HeNe) laser (SIEMENS). The intensity of the transmitted light (μW) was then recorded by the detectors at both low temperature (25 ºC, insulating phase) and high temperature (90 °C, metallic phase) to complete a cycle. Fig. 5(b) shows no noticeable change in transmitted laser intensity in both the metallic and insulator phase after 3000 continuous cycles, indicating that the solar modulation ability of the cross-linked PMMA-

VO_2 remained constant. To ensure the reliability of the test, the measurements were repeated at another two sample locations during each cycle and the results in Fig. 5(b) are the arithmetic average of the three tested points. Note that since incident light traveled across the film twice, the difference between the metallic phase (25 ºC) and the insulator phase (90 ºC) in Fig. 5(b) is approximately twice larger than that of Fig. 3(a).

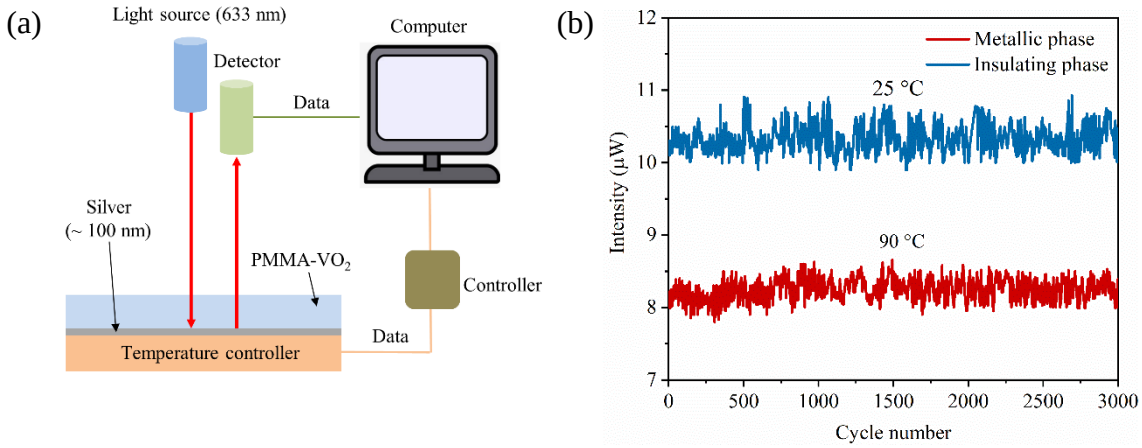

Figure 5. Fatigue test and performance of the PMMA-VO_2 film. (a) Schematic of the setup for fatigue measurements. The temperature of the insulating phase and metallic phase VO_2 were set as 25 °C and 90 ºC, respectively. (b) Variation of the transmittance of the durability enhanced PMMA-VO_2 film as a function of cycle number.

3.4 Thermal comfort and energy saving of PMMA-VO_2 film in different regions

To evaluate the energy saving performance of a PMMA-VO_2 film in different climates and regions, a heat transfer model was developed. Figure 6(a) depicts the heat and solar radiation transfer across a window pane, where the PMMA-VO_2 film with a thickness of ~ 4 μm is employed. The spectral transmittance of the PMMA-VO_2 film in both the insulating phase and the metallic phase was shown in Fig. 3(a). Since the thickness of the window is much smaller than its width

and length, the heat transfer in the *z*-direction can be treated as one-dimensional. Thus, the heat transfer in the z-direction can be described as,

$$k_{gla}\frac{d^2T(z)}{dz^2}+\nabla q(z)=0 \tag{6}$$

where k_{gla} is the thermal conductivity of the float glass, $T(z)$ is the temperature at position *z*, $q(z)$ is the local heat source carried by the solar irradiation, which can be written as

$$q(z)=\tau_{sol}I_o e^{-\beta_{gla}z} \tag{7}$$

where I_o is the incident solar energy, τ_{sol} is the solar transmittance of the PMMA-VO_2 film, and $\beta_{gla}$is the extinction coefficient of the float glass. Compared with the thickness of float glass (3 mm), the thickness of the PMMA-VO_2 (~ 4 μm) film can be ignored. Thus, the boundary conditions at $z=0$ and $z=L_{gla}$ are as follows:

$$q(z=0)=h_o(T_a-T_{z=0})+\sigma\varepsilon_o(T_a^4-T_{z=0}^4)+Q_{abs} \tag{8}$$

$$q\left(z=L_{gla}\right)=h_i\left(T_{z=L_{gla}}-T_r\right)+\sigma\varepsilon_i\left(T_{z=L_{gla}}^4-T_r^4\right) \tag{9}$$

where T_a and T_r are the external ambient temperature and the internal room temperature, respectively, h_e, h_i and $\varepsilon_e, \varepsilon_i$ are the external and internal convective heat transfer coefficients and average external and internal surface emissivities, $\sigma=5.67\times10^{-8}$ (Wm)/K^4 is the Stefan-Boltzmann's constant, $Q_{abs}=\alpha_{sol}I_o$, is the absorbed solar irradiation by the PMMA-VO_2 film, and α_{sol} is the absorbance of the PMMA-VO_2 film. Here, Eq. (6) was solved by the finite volume method [45]. The thermal conductivity and average surface emissivity of the float glass are assumed to be $k_g=0.96$ W/(mK) and $\varepsilon_o\approx0.84$ according to reference [46]. The surface emissivity of the PMMA-VO_2 film is $\varepsilon_o\approx0.9$. From Fig. 3(a), the solar transmittances (τ_{sol}) of

the PMMA-VO_2 film in the insulating phase and metallic phase are 0.57 are 0.40, respectinvely. The reflectances (r_{sol}) of the PMMA-VO_2 in both the insulating and metallic phases were measured as 0.05. Thus, the absorbance can be calculated by $\alpha_{sol} = 1 - \tau_{sol} - r_{sol}$. The inside and external convective heat transfer coefficients can be evaluated by $h_i = 3.6\ \mathrm{W/(m^2K)}$ and $h_o = (10 + 4.1v)\ \mathrm{W/(m^2K)}$, where v (m/s) is the wind speed [46]. The weather conditions including ambient temperature (T_o), window speed (v) and solar irradiation density (I_o) are acquired from the NSRDB Data Viewer [47].

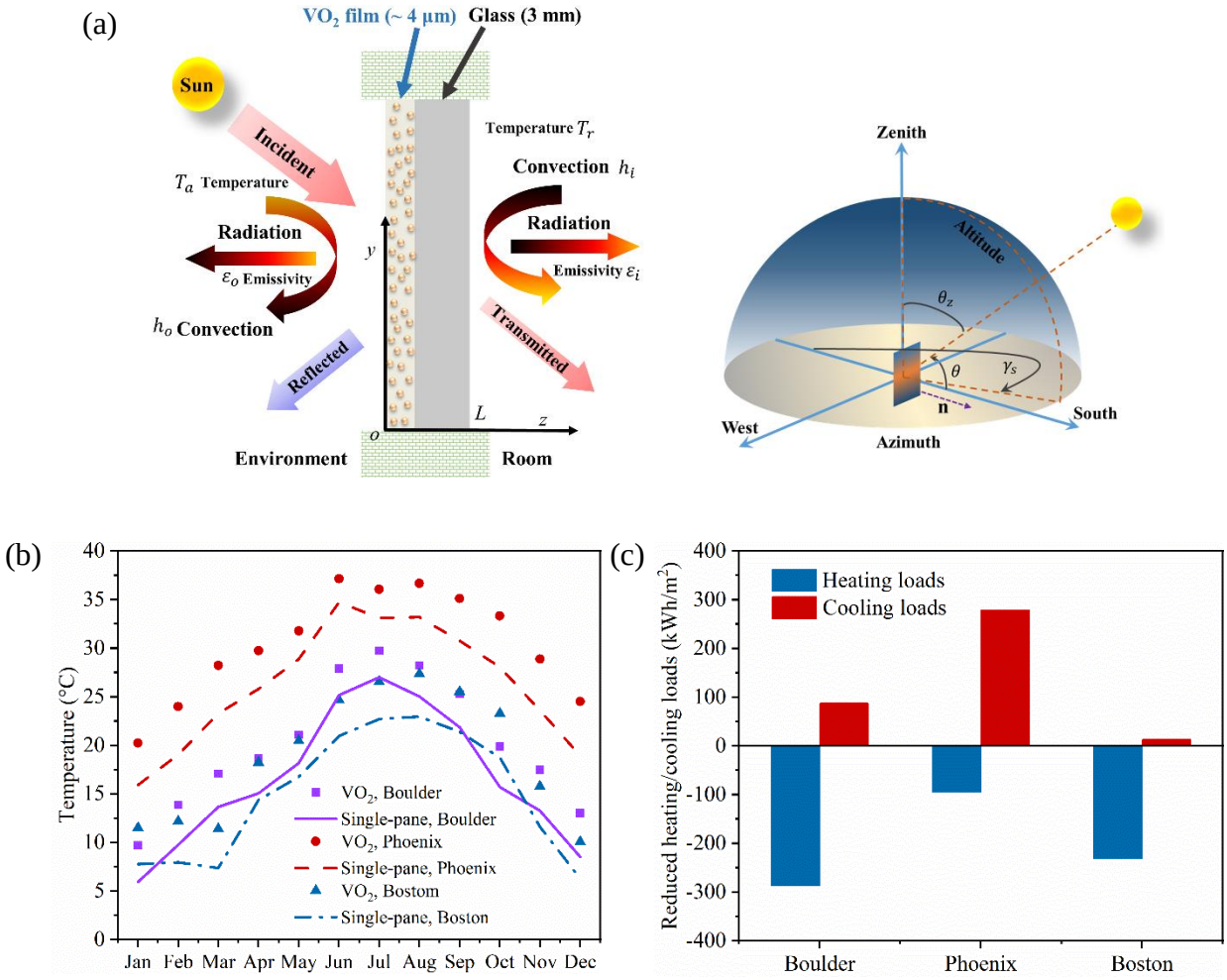

Figure 6. Thermal comfort and energy savings of the PMMA-VO_2 film in selected cities: Boulder (CO), Phoenix (AZ), and Boston (MA). (a) Schematic of heat and radiation energy transfer across

a south-facing single-pane window covered by the PMAA-VO_2 film. (b) Comparison of reduced annual heating/cooling loads of a south-facing window. (c) Influence of PMMA-VO_2 film on the inside surface temperature of a glass window.

The inside surface temperatures of the single-pane window with and without VO_2 film are compared in Fig. 6(b). After employing the PMMA-VO_2 film, the inside surface temperature of the single-pane window is ~ 5 °C higher than that of the single-pane window without a film, indicating that the PMMA-VO_2 film can reduce the temperature difference between the occupants and the innermost surface of windows, which indeed improves the thermal comfort and condensation resistance of the single-pane window in cold climates significantly [48]. Since the solar transmittance of the PMMA-VO_2 film (0.57 ~ 0.4, Fig. 3(a)) is smaller than the single-pane window (~ 90%), applying the PMMA-VO_2 film increase the heating loads in cold climates and reduce the cooling loads in hot climates. Figure 6 (c) compares the reduced annual heating/cooling loads of a south-facing window in different regions. In this Figure, the positive/negative sign represents the reduced/increased energy. For simplicity, it is assumed that the transmitted solar energy decreases (increases) the heating (cooling) loads when the external ambient temperature is higher (lower) than the internal room temperature (21 ºC). Note that the transmitted solar energy includes both the directly transmitted solar irradiation and the absorbed solar energy by window pane and subsequently transferred towards the indoor room environment through heat conduction. Clearly, the cooling demands in the hot areas (e.g., Phoenix) are significantly reduced. However, in the cold areas (e.g., Boston), the increased heating loads in winter are much higher than the reduced cooling loads in summer, indicating that the PMMA-VO_2 film could increase the annual energy cost.

IV. Conclusions

In summary, a thermochromic film based on vanadium dioxide (VO_2) nanoparticles and poly (methyl methacrylate) (PMMA) matrix was proposed and fabricated using the blade coating method. The area and thickness of the fabricated film are 600 mm × 300 mm (length × width) and ~ 4 μm, respectively. It is shown that the PMMA-VO_2 film has a luminous transmittance of ~ 50%, solar modulation ability of ~ 17.1%, and haze of ~ 11%. The solar modulation ability of the PMMA-VO_2 film is higher than that of most previous studies which are usually smaller than 10%. The lifetime of the VO_2 nanoparticles is greatly improved by the cross-linked polymer matrix with high molecular weight. The durability tests were performed in the accelerated aging chamber whose environmental temperature is 60 °C, and humidity is ~ 95%. It was shown that the lifetime of the VO_2 nanoparticles embedded in the cross-linked PMMA matrix with molecular weight ~ 950,000 is ~ 900 hours, which is much longer than that (~ 200 hours) of the VO_2 in the non-cross-linked PMMA matrix with low molecular weight (~ 15,000). The lifetime of the VO_2 nanoparticles in the highly entangled and cross-linked polymer matrix is close to or longer than the lifetime of thermochromic films made of VO_2 protected by environmental stable materials (e.g., aluminum oxide and SiN_x), indicating that cross-linked the polymer chains with high molecular weight could improve the durability of VO_2 remarkably. It was shown that there is no decay of the solar modulation ability after ~ 3000 cycles of fatigue test. The analysis also shows that the PMMA-VO_2 film could greatly reduce the cooling demands in hot climates and improve the thermal comfort in cold climates.

Acknowledgments

X. Zhao and S. Mofid acknowledge the help of Dr. L. Shen., Dr. Y. Zai and Mr. A. Aili on the synthesis of VO_2 nanoparticles and the fabrication of PMMA-VO_2 films, Mr. H. Zhao. and Prof.

G. Cao on the XRD measurements, Mr. D. Alchenberger and Mr. M. Cart from JILA Keck lab on the SEM and optical characterization and Mrs. B. Cunningham for schematics and illustrations. The involvement of researchers from Norway has been supported by the Research Council of Norway through the SINTEF and NTNU research project" High-Performance Nano Insulation Materials" (Hi-Per NIM, project no. 250159) within the NANO2021 program. Furthermore, the Research Council of Norway is acknowledged for the support to the" Norwegian Micro- and Nano-Fabrication Facility" (NorFab, project no. 245963/F50).

Author Contributions

R.Y., X.Y. and B.P.J. designed the research. S.A.M. and X.Y. conceived the experiments, characterization, and modeling. X.Z., S.A.M., T.G., G.T., B.P.J., X.Y, and R.Y. wrote the manuscript. All authors participated in the discussion of the research.

Declaration of Interests

The authors declare no conflict of interest.

References

[1] K. Ismail, J. Henríquez, Thermally effective windows with moving phase change material curtains, Applied Thermal Engineering, 21 (2001) 1909-1923.
[2] R.C. Temps, K. Coulson, Solar radiation incident upon slopes of different orientations, Solar Energy, 19 (1977) 179-184.
[3] Y. Wang, E.L. Runnerstrom, D.J. Milliron, Switchable materials for smart windows, Annual Review of Chemical and Biomolecular Engineering, 7 (2016) 283-304.
[4] H.N. Kim, S. Yang, Responsive Smart Windows from Nanoparticle-Polymer Composites, Advanced Functional Materials, (2019) 1902597.
[5] Y. Ke, C. Zhou, Y. Zhou, S. Wang, S.H. Chan, Y. Long, Emerging thermal- responsive materials and integrated techniques targeting the energy- efficient smart window application, Advanced Functional Materials, 28 (2018) 1800113.
[6] Y. Cui, Y. Ke, C. Liu, Z. Chen, N. Wang, L. Zhang, Y. Zhou, S. Wang, Y. Gao, Y. Long, Thermochromic VO_2 for energy-efficient smart windows, Joule, (2018).
[7] Z. Chen, Y. Gao, L. Kang, C. Cao, S. Chen, H. Luo, Fine crystalline VO_2 nanoparticles: synthesis, abnormal phase transition temperatures and excellent optical properties of a derived VO_2 nanocomposite foil, Journal of Materials Chemistry A, 2 (2014) 2718-2727.

[8] Y. Chen, X. Zeng, J. Zhu, R. Li, H. Yao, X. Cao, S. Ji, P. Jin, High performance and enhanced durability of thermochromic films using VO_2@ ZnO core–shell nanoparticles, ACS Applied Materials & Interfaces, 9 (2017) 27784-27791.
[9] S.-Y. Li, G.A. Niklasson, C.-G. Granqvist, Nanothermochromics: calculations for VO_2 nanoparticles in dielectric hosts show much improved luminous transmittance and solar energy transmittance modulation, Journal of Applied Physics, 108 (2010) 063525.
[10] Y. Gao, S. Wang, H. Luo, L. Dai, C. Cao, Y. Liu, Z. Chen, M. Kanehira, Enhanced chemical stability of VO_2 nanoparticles by the formation of SiO_2/VO_2 core/shell structures and the application to transparent and flexible VO_2-based composite foils with excellent thermochromic properties for solar heat control, Energy & Environmental Science, 5 (2012) 6104-6110.
[11] Y. Li, S. Ji, Y. Gao, H. Luo, P. Jin, Modification of Mott phase transition characteristics in VO_2@ TiO_2 core/shell nanostructures by misfit-strained heteroepitaxy, ACS Applied Materials & Interfaces, 5 (2013) 6603-6614.
[12] L. Zhao, L. Miao, C. Liu, C. Li, T. Asaka, Y. Kang, Y. Iwamoto, S. Tanemura, H. Gu, H. Su, Solution-processed VO_2-SiO_2 composite films with simultaneously enhanced luminous transmittance,solar modulation ability and anti-oxidation property, Scientific reports, 4 (2014) 7000.
[13] R. Lindström, V. Maurice, S. Zanna, L. Klein, H. Groult, L. Perrigaud, C. Cohen, P. Marcus, Thin films of vanadium oxide grown on vanadium metal: oxidation conditions to produce V_2O_5 films for Li-intercalation applications and characterisation by XPS, AFM, RBS/NRA, Surface and Interface Analysis, 38 (2006) 6-18.
[14] Y.-X. Ji, S.-Y. Li, G.A. Niklasson, C.G. Granqvist, Durability of thermochromic VO_2 thin films under heating and humidity: effect of Al oxide top coatings, Thin Solid Films, 562 (2014) 568-573.
[15] T. Chang, X. Cao, L.R. Dedon, S. Long, A. Huang, Z. Shao, N. Li, H. Luo, P. Jin, Optical design and stability study for ultrahigh-performance and long-lived vanadium dioxide-based thermochromic coatings, Nano Energy, 44 (2018) 256-264.
[16] K. Tong, R. Li, J. Zhu, H. Yao, H. Zhou, X. Zeng, S. Ji, P. Jin, Preparation of VO_2/Al-O core-shell structure with enhanced weathering resistance for smart window, Ceramics International, 43 (2017) 4055-4061.
[17] Y. Li, S. Ji, Y. Gao, H. Luo, M. Kanehira, Core-shell VO_2@TiO_2 nanorods that combine thermochromic and photocatalytic properties for application as energy-saving smart coatings, Scientific Reports, 3 (2013) 1370.
[18] S. Long, X. Cao, N. Li, Y. Xin, G. Sun, T. Chang, S. Bao, P. Jin, Application-oriented VO_2 thermochromic coatings with composite structures: optimized optical performance and robust fatigue properties, Solar Energy Materials and Solar Cells, 189 (2019) 138-148.
[19] A. Huang, Y. Zhou, Y. Li, S. Ji, H. Luo, P. Jin, Preparation of $V_xW_{1-x}O_2$(M)@SiO_2 ultrathin nanostructures with high optical performance and optimization for smart windows by etching, Journal of Materials Chemistry A, 1 (2013) 12545-12552.
[20] Ö. Pekcan, Ş. Uğur, Molecular weight effect on polymer dissolution: a steady state fluorescence study, Polymer, 43 (2002) 1937-1941.
[21] L.H. Sperling, Introduction to physical polymer science, John Wiley & Sons, 2005.
[22] K. Balani, V. Verma, A. Agarwal, R. Narayan, Physical, Thermal, and Mechanical Properties of Polymers, in, John Wiley & Sons, Inc, Hoboken, NJ, United States, 2014.
[23] L. Tan, F. Yang, M.R. Kim, P. Li, D.T. Gangadharan, J.l. Margot, R. Izquierdo, M. Chaker, D. Ma, Enhanced long-term and thermal stability of polymer solar cells in air at high humidity with the formation of unusual quantum dot networks, ACS Applied Materials & Interfaces, 9 (2017) 26257-26267.
[24] S.C. George, S. Thomas, Transport phenomena through polymeric systems, Progress in Polymer Science, 26 (2001) 985-1017.
[25] A. Berens, H. Hopfenberg, Diffusion of organic vapors at low concentrations in glassy PVC, polystyrene, and PMMA, Journal of Membrane Science, 10 (1982) 283-303.
[26] M. Klinger, L.P. Tolbod, K.V. Gothelf, P.R. Ogilby, Effect of polymer cross-links on oxygen diffusion in glassy PMMA films, ACS Applied Materials & Interfaces, 1 (2009) 661-667.

[27] M. Li, S. Magdassi, Y. Gao, Y. Long, Hydrothermal synthesis of VO_2 polymorphs: advantages, challenges and prospects for the application of energy efficient smart windows, Small, 13 (2017) 1701147.
[28] W. Li, S. Ji, Y. Li, A. Huang, H. Luo, P. Jin, Synthesis of VO_2 nanoparticles by a hydrothermal-assisted homogeneous precipitation approach for thermochromic applications, RSC Advances, 4 (2014) 13026-13033.
[29] R. Li, S. Ji, Y. Li, Y. Gao, H. Luo, P. Jin, Synthesis and characterization of plate-like VO_2 (M)@SiO_2 nanoparticles and their application to smart window, Materials Letters, 110 (2013) 241-244.
[30] U. Ali, K.J.B.A. Karim, N.A. Buang, A review of the properties and applications of poly (methyl methacrylate)(PMMA), Polymer Reviews, 55 (2015) 678-705.
[31] D.J. Carbaugh, J.T. Wright, R. Parthiban, F. Rahman, Photolithography with polymethyl methacrylate (PMMA), Semiconductor Science and Technology, 31 (2015) 025010.
[32] C. Wochnowski, M.S. Eldin, S. Metev, UV-laser-assisted degradation of poly (methyl methacrylate), Polymer Degradation and Stability, 89 (2005) 252-264.
[33] H. Albeladi, A. Al-Romaizan, M. Hussein, Role of cross-linking process on the performance of PMMA, Int. J. Biosens. Bioelectron, 3 (2017) 279-284.
[34] S. Eve, J. Mohr, Study of the surface modification of the PMMA by UV-radiation, Procedia Engineering, 1 (2009) 237-240.
[35] M.M. Qazilbash, M. Brehm, B.-G. Chae, P.-C. Ho, G.O. Andreev, B.-J. Kim, S.J. Yun, A. Balatsky, M. Maple, F. Keilmann, Mott transition in VO_2 revealed by infrared spectroscopy and nano-imaging, Science, 318 (2007) 1750-1753.
[36] Y. Kim, S. Yu, J. Park, D. Yoon, A.M. Dayaghi, K.J. Kim, J.S. Ahn, J. Son, High-throughput roll-to-roll fabrication of flexible thermochromic coatings for smart windows with VO_2 nanoparticles, Journal of Materials Chemistry C, 6 (2018) 3451-3458.
[37] M.A. Hussein, R.M. El-Shishtawy, B.M. Abu-Zied, A.M. Asiri, The impact of cross-linking degree on the thermal and texture behavior of poly (methyl methacrylate), Journal of Thermal Analysis and Calorimetry, 124 (2016) 709-717.
[38] G. Wyszecki, W.S. Stiles, Color science, Wiley New York, 1982.
[39] C. Riordan, R. Hulstron, What is an air mass 1.5 spectrum?(Solar cell performance calculations), in: IEEE Conference on Photovoltaic Specialists, IEEE, 1990, pp. 1085-1088.
[40] ASTM D1003-13-Standard test method for haze and luminous transmittance of transparent, ASTM International West Conshohocken, 2013.
[41] C.F. Bohren, D.R. Huffman, Absorption and scattering of light by small particles, John Wiley & Sons, 2008.
[42] B.J. Park, M.S. Kim, H.J. Choi, Fabrication and magnetorheological property of core/shell structured magnetic composite particle encapsulated with cross-linked poly (methyl methacrylate), Materials Letters, 63 (2009) 2178-2180.
[43] B.P. Jelle, Accelerated climate ageing of building materials, components and structures in the laboratory, Journal of Materials Science, 47 (2012) 6475-6496.
[44] B.P. Jelle, E. Sveipe, E. Wegger, A. Gustavsen, S. Grynning, J.V. Thue, B. Time, K.R. Lisø, Robustness classification of materials, assemblies and buildings, Journal of Building Physics, 37 (2014) 213-245.
[45] R. Eymard, T. Gallouët, R. Herbin, Finite volume methods, Handbook of Numerical Analysis, 7 (2000) 713-1018.
[46] B.P. Jelle, Solar radiation glazing factors for window panes, glass structures and electrochromic windows in buildings-Measurement and calculation, Solar Energy Materials and Solar Cells, 116 (2013) 291-323.
[47] https://maps.nrel.gov/nsrdb-viewer/.
[48] P. Lyons, D. Arasteh, C. Huizenga, Window performance for human thermal comfort, Transactions-American Society of Heating Refrigerating and Air Conditioning Engineers, 106 (2000) 594-604.

- The highly entangled and crosslinked PMMA matrix was used to improve the lifetime of VO_2 nanoparticles.
- The PMMA-VO_2 thermochromic film shows a high luminous transmittance of ~ 50% and solar modulation ability of ~ 17%.
- No noticeable decay of the solar modulation ability was observed after ~ 3000 cycles of fatigue test.
- The proposed method provides a promising pathway toward environmentally stable and easily scalable thermochromic film.

Graphical Abstract

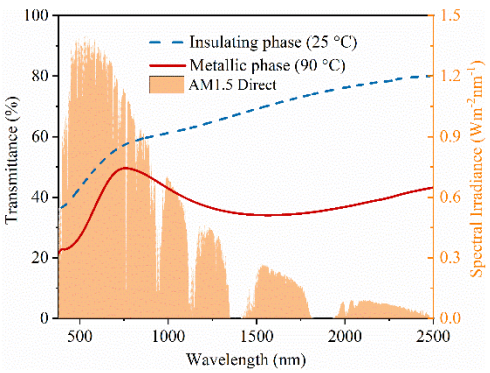

Durability-Enhanced VO_2 Thermochromic Film for Smart Windows

Xinpeng Zhao[2,#], Sohrab A. Mofid[2,3,#], Tao Gao[3], Gang Tan[4], Bjørn Petter Jelle[3,5,*], Xiaobo Yin[2,*], and Ronggui Yang[1,*]

[1]School of Energy and Power Engineering, Huazhong University of Science and Technology, Wuhan, Hubei 430074, China.

[2]Department of Mechanical Engineering, University of Colorado, Boulder, Colorado 80309, USA.

[3]Department of Civil and Environmental Engineering, Norwegian University of Science and Technology (NTNU), NO-7491 Trondheim, Norway.

[4] Department of Civil and Architectural Engineering, University of Wyoming, Laramie, Wyoming 82071, USA.

[5]Department of Materials and Structures, SINTEF Community, NO-7465 Trondheim, Norway.

# These authors contribute equally.

*E-mail: ronggui@hust.edu.cn

xiaobo.yin@colorado.edu

bjorn.petter.jelle@ntnu.no

Abstract

Vanadium dioxide (VO_2) based thermochromic films are of great interest for energy-saving smart windows as they can dynamically change the solar transmittance as the ambient temperature changes. However, VO_2 is thermodynamically unstable and could be easily oxidized by the oxygen and moisture in the ambient air. In this work, a durability-enhanced VO_2 nanoparticle-polymer thermochromic film was proposed and fabricated using the blade coating method where the cross-linked and highly entangled poly (methyl methacrylate) (PMMA) chain with molecular weight (~

950,000) was adopted to block gas diffusion in the polymer matrix. It was shown that the developed VO_2 nanoparticles film kept ~ 30% of the solar modulation ability after ~ 900 hours of accelerated durability test in the aging environment with a temperature at 60 ºC and ~ 95% humidity. This is ~ 4 times of the lifetime of the VO_2 nanoparticles which are embedded in the non-cross-linked PMMA matrix with low molecular weight (~ 15,000). The cross-linked PMMA-VO_2 film also showed a high luminous transmittance of ~ 50%, a high solar modulation ability of ~17% and a low haze of ~ 11%. Our method provides an easy and effective strategy to improve the lifetime of VO_2 nanoparticles, showing a promising pathway toward environmentally stable and easily scalable thermochromic films for energy-efficient smart windows.

Keywords: Vanadium dioxide nanoparticle, Cross-linking, Thermochromic, Smart window.

I. Introduction

With a high solar transmittance > 90%, as much as ~ 800 W/m^2 solar irradiation reaches the indoor environment through windows during daytime [1, 2]. The transmitted solar energy greatly reduces the energy consumption for heating in cold climates. However, excessive solar heating would result in increased cooling loads in hot climates, especially in summer. Smart windows that could dynamically adjust the transmittance of solar irradiation have been thought of as one of the most promising techniques to reduce the energy consumption of buildings [3, 4]. In particular, there are a lot of interests in vanadium dioxide (VO_2) nanoparticle and transparent polymer matrix based thermochromic films in recent years, especially due to the relatively high luminous transmittance of ~ 50%, and solar modulation ability of ~ 20% [5-11]. However, pristine VO_2 is thermodynamically unstable and can be easily oxidized to V_2O_5 when exposed to air for several months [12, 13], which in turn dramatically reduces the solar modulation ability. A humid environment would also greatly accelerate the oxidation process. Previous studies [8, 14-16]

showed that the thermochromic performance of VO_2 decreased noticeably when exposed to relatively high humidity for only ~ 24 hours, deterring the practical deployment of VO_2 based smart windows.

To improve the anti-oxidation ability and increase the lifetime of VO_2 nanoparticles, core-shell nanoparticles have been proposed, where the environmentally stable materials are used as a protection layer to prevent VO_2 from water and oxygen exposure and hence to decrease the oxidation rate. For example, the previous study showed that employing aluminum oxide based shells could increase the lifetime of VO_2 from ~ 3 days to more than ~ 20 days under accelerated aging tests with a 60 ºC temperature and 90% relative humidity[16]. In addition, other environmentally stable oxides like SiO_2 [10], TiO_2 [17], and ZnO [8] have been used to increase the durability of VO_2 nanoparticles. However, in practical applications, when VO_2 nanoparticles transit periodically from monoclinic (M, $a_M = 5.75, b_M = 4.52$ Å, $c_M = 5.38$ Å, $\beta = 122.6°$) structure to tetragonal rutile (R, $a_R = b_R = 4.55$ Å, $c_R = 2.86$ Å) structure [6], the interface stress between the VO_2 cores and oxide protection shells induced by the lattice structure transformation of VO_2 nanoparticles may result in the formation of micro cracks at the interface. A recent study [18] has shown that cracks occur in VO_2 based multilayer thin films after ~ 1000 times of reversible phase transitions. In addition, cracks were even found in SiO_2 [19] and TiO_2 shells [8, 17] during the synthesis process. The accelerated aging tests at a temperature of 60 ºC and 90% relative humidity showed that the lifetime of the SiO_2 coated VO_2 nanoparticles were only ~ 72 hours due to the appearance of such cracks [8]. It is also worthwhile to note that although the introduction of a shell layer potentially enhances the durability of VO_2 nanoparticles and improves the solar luminous transmittance, it may lower the solar modulation ability of the film. For example, the experimental results by Li *et al.* showed that the solar modulation ability decreased ~ 50% when

the VO_2 nanoparticles were coated by ~ 7 nm thick TiO_2 shells [17]. Besides the core-shell nanoparticle structures, blocking the diffusion of oxygen and moisture in the polymer matrix may also delay the oxidation process of VO_2 nanoparticles. In general, increasing the molecular weight (length) of polymer chain and generating chemical crosslinks between neighboring polymer chains are two effective ways to reduce gas diffusion in polymer matrix because the mobility of polymer chains can be restricted by the highly entangled polymer chains and the ionic or covalent bonds between neighboring polymer chains [20-24]. A previous study by Berens *et al.* showed that the diffusivity of organic vapors (e.g., $(CH_3)_2CO$, $CHCl_3$) was decreased by a factor of ~ 10 when the molecular weight of polystyrene increased from 10,000 to 300,000 [25]. Klinger *et al.* showed that a 0.45% mole percentage of cross-linking in poly(methyl methacrylate) (PMMA) could reduce the oxygen diffusion coefficient by ~ 30% [26]. These together imply that highly cross-linked high molecular weight polymers may provide a simple and yet effective pathway to protect the randomly dispersed VO_2 nanoparticles from oxidation.

Considering the high transparency, structural stability, and easy to crosslink, a cross-linked high molecular weight PMMA film (~ 950,000) embedded with VO_2 nanoparticles with a size of 50 ~ 80 nm was demonstrated in this work. The developed PMMA-VO_2 film with a thickness of ~ 4 μm has a relatively high luminous transmittance of ~ 50%, solar modulation ability of ~17.1%, and a low haze value of ~ 11%. The accelerated aging test at a temperature of 60 ºC and a relative humidity of ~ 95% showed that the lifetime of the VO_2 nanoparticles dispersed in the cross-linked high molecular weight PMMA film (~ 950,000) is more than 900 hours, which is much longer than that of VO_2 nanoparticles in the non-cross-linked low molecular weight (~ 15,000) PMMA, around 200 hours. The lifetime of VO_2 nanoparticles in the cross-linked and entangled PMMA matrix is significantly longer than the reported VO_2 nanoparticles coated by SiO_2 (~ 72 hours) ,

$Al(OH)_3$ (~ 120 hours) , and VO_2 thin film protected by Al_2O_3 (~ 100 hours) [14], and is comparable to the VO_2 nanoparticles coated by Al_2O_3 (> 480 hours) [16], and VO_2 thin film protected by SiN_x (~ 600 hours) [18]. The fatigue test shows that the thermochromic performance of the developed PMMA-VO_2 films keeps the same after 3000 times of continuous reversible phase transitions. The analysis also shows that the developed PMMA-VO_2 film could greatly reduce the cooling demands in hot climates and improve the thermal comfort and condensation resistance in cold climates.

II. Materials and methods

2.1 Synthesis

2.1.1 Chemicals and materials

Vanadium pentoxide (V_2O_5, 99.99%, Sigma Aldrich), oxalic acid dihydrate ($H_2C_2O_4 \cdot 2H_2O$, 99%, Sigma Aldrich), poly (methyl methacrylate) (PMMA, molecular weight ~15,000 (15K), Sigma Aldrich), and anisole (C_7H_8O, 99.7%, Sigma Aldrich), PMMA A4 (molecular weight ~950,000 (950K), MicroChem Corp) resists in anisole were purchased and used as as-supplied without additional purifications.

2.1.2 Synthesis of monoclinic *VO_2 (M)*

Various synthesis methods of monoclinic VO_2 (M) could be found in the earlier studies [8, 10, 27-29]. In this work, VO_2 nanoparticles were synthesized by the hydrothermal method [8]. For a typical synthesis, 2.0 g of V_2O_5 powder was added to 40.0 ml deionized water and was stirred for 20 min, then 3.4 g of oxalic acid dihydrate was added to the mixture and further stirred until a clear light green/blue slurry was formed. The suspension was then moved to a 150 ml Teflon-lined stainless-steel autoclave. The autoclave was kept at 260 °C for 24.0 h and then air-cooled to room

temperature. The resulting black-precipitates was collected and washed with deionized water and ethanol 3 times, respectively, then dried with a vacuum furnace at 120 °C for 5.0 h. A schematic illustrating the synthesis process could be found in Fig. 1(a).

2.2 Measurements

The commercial Netzsch differential scanning calorimetry (DSC 204 F1 Phoenix) was used to determine the phase transition properties of the synthesized VO_2 powder over the temperature range from 0 to 100 °C, and the heat absorption properties of the PMMAs from 0 to 550 °C, respectively. The heating/cooling rate was set at 10 °C/min. The crystalline phase of the VO_2 powder was identified using X-ray diffraction (XRD, MiniFlex600, Rigaku, Japan) with Cu Kα radiation (λ = 1.5418) at a voltage 40 kV and a current of 40 mA. Transmission electron microscope (TEM, JEM-2010) was used to characterize the morphology and microstructure of the nanoparticles. Optical performance, including spectral transmittance and haze of the films, was measured using a UV-Vis-Near-IR spectrophotometer (Shimadzu UV-3101) together with a temperature control unit including black anodized aluminum 6061 plate, and a variac (2 A, 120 V). A helium-neon (HeNe) laser (SIEMENS), and a programmable stage temperature controller (LINKAM TMS 94) together with a heating/freezing microscope stage (LINKAM MDS600) with a microscope objective lens (NIKON, Plan Fluor ELWD 20x/0.45) was assembled to measure the reflectance spectrum of the film with a 200 nm silver coating in 633 nm at 25 °C and 90 °C with ramping rate 10 °C/min. A TPS (TENNEY) environmental chamber was used to create a steady-state temperature and humidity (60 °C, relative humidity ~ 95%) for the durability testing of the PMMA-VO_2 films.

III. Results and discussion

3.1 Fabrication and characterization of PMMA-VO_2 film

PMMA is a non-toxic, inexpensive thermoplastic with high optical transparency, high mechanical strength and durability, excellent thermal stability, and weather resistance [30]. PMMA with different molecular weights (chain length and entanglement) could be obtained and processed easily [31]. Moreover, the influence of the near-UV from solar radiation on the PMMA is minor since PMMA is only sensitive to high energy radiation such as the electron beam, x-rays, and UV radiation with wavelengths shorter than 300 nm [31, 32]. Thus, PMMA was adopted as the polymer matrix in this work. As shown in Fig. 1(b), the desired amount of as-synthesized crystalline monoclinic VO_2 nanoparticles was dispersed ultrasonically into 40 ml of PMMA 950K A4. The solution was then stirred at room temperature for 12 hours. Generally, the molecule chains of PMMA could be interlinked using several methods, including free radical polymerization, condensation reactions, small molecule crosslinking, and radiation [33]. Wochnowski *et al*. showed that the 248nm-wavelength ultraviolet (UV) irradiation could crosslink the two neighboring PMMA molecules by establishing an oxygen bridge between *ester* side chains or connecting the two *carbonyl* groups [32]. The degree of crosslinking of the PMMA matrix could be controlled by both the dose and the duration of the UV irradiation. A higher degree of crosslinking usually has a higher endothermic peak, which can be evaluated by the DSC measurements. The radiation dose needs to be smaller than 2.0 J/cm^2 to prevent the brittleness of PMMA film after crosslinking [34]. Here the PMMA/VO_2 solution was irradiated by the UV radiation (220 ~380 nm, ADJ Products) for 10 hours in the room environment while being stirred at 300 rpm to generate crosslinks in the PMMA matrix. The final mixture was maintained at a constant temperature of ~ 75 °C on a hotplate for 40 min. The solution was then loaded onto a ~ 50 μm thick transparent and chemically stable biaxially-oriented polyethylene terephthalate (BoPET) sheet laminated on a piece of float glass using blade coating method as shown in Fig.

1(b). The final thickness of the dried PMMA-VO_2 film is determined by the concentration of PMMA, the moving speed of the blade, and the gap between the blade tip and the substrate. Here the film was formed using blade coating at a speed of 15mm/s. After the wet film is fabricated, the film is dried in a fume hood for 2 hours. Finally, a thin film with an area of 600 mm × 300 mm (length × width) and a thickness of ~ 4 μm is obtained as shown in Fig. 1(c), in which the PMMA-VO_2 film is coated on a 50 μm thick BoPET film. No obvious variation of the film brittleness was observed.

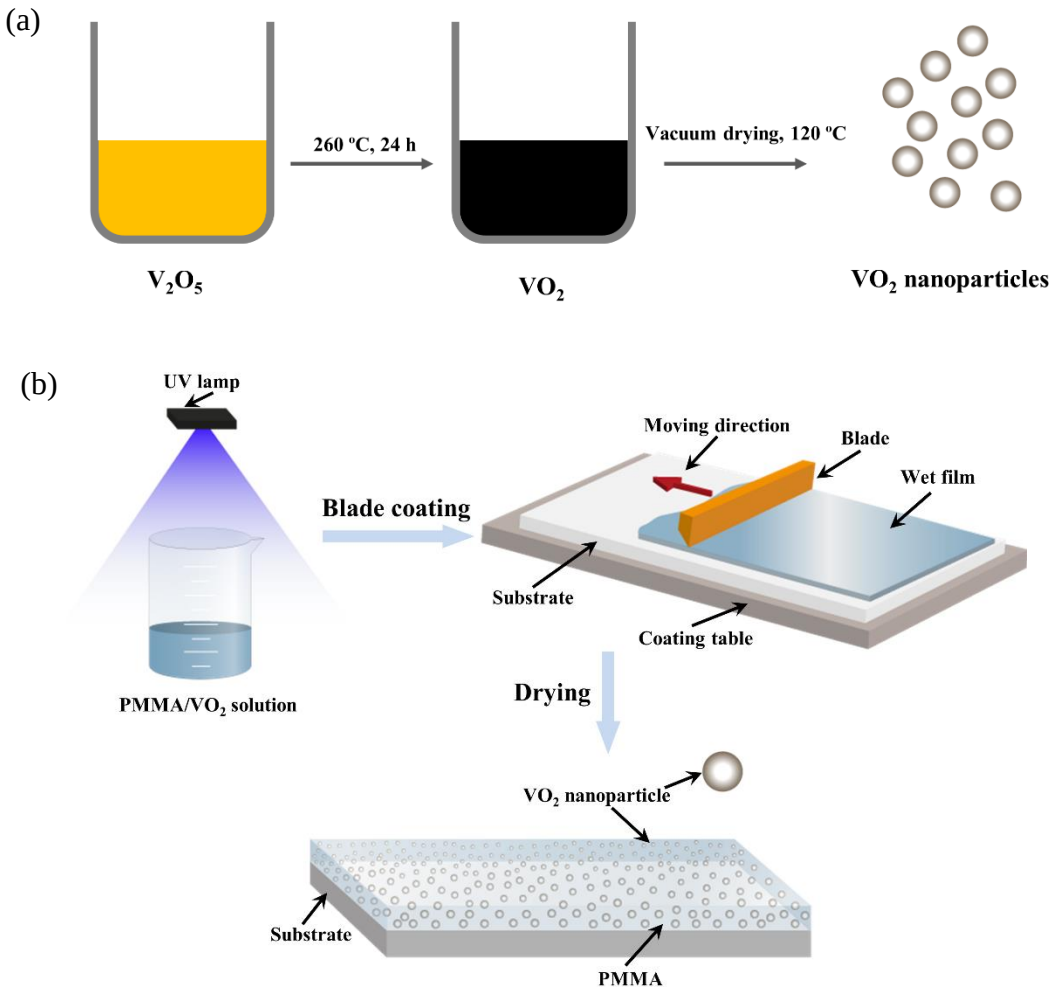

(c) 

Figure 1. Fabrication of durability-enhanced PMMA-VO_2 thermochromic film for smart windows. (a) Synthesis process of VO_2 nanoparticles using the hydrothermal method. (b) Schematic of the fabrication process of the meter-scale durability-enhanced PMMA-VO_2 film using the blade coating method. The PMMA/VO_2 solution was first exposed to ultraviolet (UV) rays. Then, the wet PMMA-VO_2 film was fabricated using the blade coating method. After drying, the PMMA-VO_2 composite film was obtained. (c) Snapshot of a PMMA-VO_2 film with a size of 600 mm × 300 mm (length × width) manufactured using the blade coating method, in which a ~ 4.0 μm thick PMMA-VO_2 film is coated on a 50 μm thick BoPET film.

Figure 2(a) shows the morphology of VO_2 nanoparticles from transmission electron microscopy (TEM). It is seen that most of the nanoparticles have an approximately spherical shape, and the diameter of the VO_2 nanoparticles mainly lies in the range of 50 ~ 80 nm. Fig. 2(b) presents the X-Ray Diffraction (XRD) measurement of the VO_2 nanoparticles, where the diffraction peaks indicate that the VO_2 nanoparticles are in the monoclinic phase (M2, C2/m) [12]. The phase transition temperature of the VO_2 nanoparticles was determined by differential scanning calorimetry (DSC) measurements using a heating/cooling rate of 10 ºC/min in the temperature

range from 0 to 110 °C. Since the insulator-to-metal transformation of VO_2 is a first-order phase transition [35], the discontinuous variation of entropy results in the release or absorption of latent heat. As shown in Fig. 2 (c), when VO_2 transits from the monoclinic (M) insulator phase to the rutile (R) phase during the heating cycle, an endothermic (positive) peak with peak temperature ~ 71 °C is observed. A corresponding exothermic (negative) peak, representing metal-to-insulator transition, occurs in the cooling cycle, where the peak temperature is ~ 63 ºC. This DSC curve is similar to those reported in the literature [8, 11, 36]. Since the crosslinking process could generate new chemical bonding between neighboring chains, the cross-linked PMMA polymers are expected to have a higher endothermic peak and a larger maximum decomposition temperature [37]. Figure 2(d) compares the DSC thermographs of cross-linked PMMA and non-cross-linked PMMA with molecular weight ~ 950,000. Comparing to the non-UV exposed 950,000 PMMA, the 950,000 PMMA under UV exposure has a higher endothermic peak (from ~ 6.0 μV/mg to ~ 9.5 μV/mg) and a larger maximum decomposition temperature (from 375 ºC to 386 ºC), indicating the crosslinks were generated.

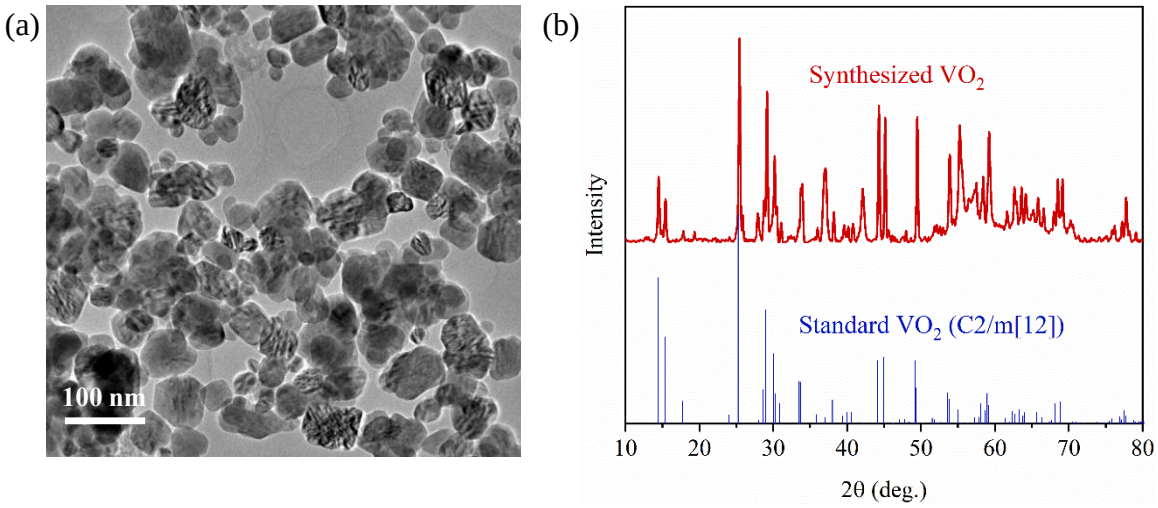

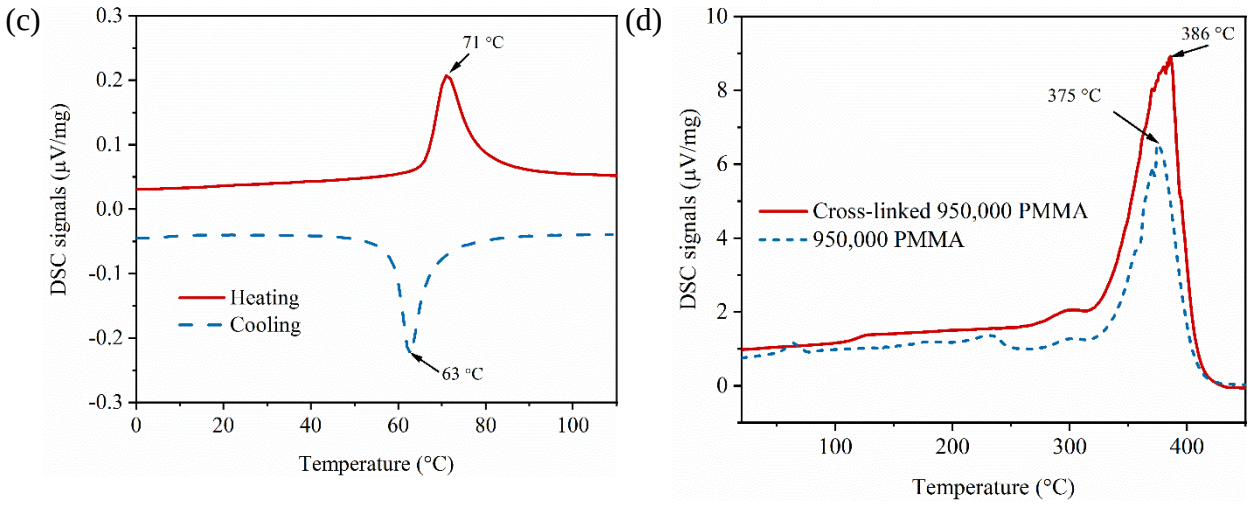

Figure 2. Characterization of the synthesized VO_2 nanoparticles. (a) Transmission electron microscopy (TEM) image of the VO_2 nanoparticles. (b) X-Ray Diffraction (XRD) pattern of the VO_2 nanoparticles. (c) Differential scanning calorimetry (DSC) of the VO_2 nanoparticles, where the heating/cooling rate is set at 10 ºC/min. (d) Comparison of the DSC thermograms of the cross-linked and non-cross-linked PMMA with molecular weight ~ 950,000. The positive peak represents an endothermic process, and the negative peak represents an exothermic process.

3.2 Optical performances of PMMA-VO_2 film

To evaluate the thermochromic performance of the PMMA-VO_2 film, the total transmittance and haze, were both measured using a commercial UV-Vis-Near-IR spectrophotometer (Shimadzu UV-3101). The total transmittance ($\tau_{\lambda,tot}$) were measured by placing the PMMA-VO_2 film and a diffuse reflector at the inlet and outlet of the integrating sphere, respectively. The measured total spectral transmittances of the PMMA-VO_2 film at low temperature (~ 25 ºC) and high temperature (~ 90 °C) are shown in Fig. 3(a). Since the metallic phase VO_2 blocks the near-infrared (NIR) solar radiation, it was found that the transmittance of the PMMA-VO_2 in the range of 800 ~ 2500 nm was much smaller when the temperature of the

PMMA-VO_2 film was set at ~ 90 ºC. The mean luminous (380-780 nm) transmittance τ_{lum} and mean solar (280-2500 nm) transmittance τ_{sol} were then calculated as,

$$\tau_{lum} = \frac{\int_{380\ nm}^{780\ nm} I_{lum,\lambda}\tau_{\lambda,tot}d\lambda}{\int_{380\ nm}^{780\ nm} I_{lum,\lambda}d\lambda} \quad (1)$$

$$\tau_{sol} = \frac{\int_{280\ nm}^{2500\ nm} I_{sol,\lambda}\tau_{\lambda,tot}d\lambda}{\int_{280\ nm}^{2500\ nm} I_{sol,\lambda}d\lambda} \quad (2)$$

where $I_{lum,\lambda}$ is the standard luminous efficiency function for vision [38], $I_{sol,\lambda}$ is the solar radiation intensity of air mass 1.5 (AM1.5) corresponding to the sun standing 37° above the horizon [39], and $\tau_{\lambda,tot}$ is the total transmittance of radiation at wavelength λ shown in Fig. 3(a). The solar modulation ability $\Delta\tau_{sol}$ is defined by the difference of solar transmittance before and after the phase transition, *i.e.*,

$$\Delta\tau_{sol} = \tau_{sol}(T < T_c) - \tau_{sol}(T > T_c) \quad (3)$$

where T_r is the critical phase change temperature of VO_2. According to Eqs. (1-2), the luminous transmittance at low temperature and solar modulation ability are calculated to be ~ 50% and ~17.1%, respectively. Besides, we have also checked the uniformity of the coating by measuring the transmittance of the film at several different locations. The difference of the solar transmittances among different points was found to be smaller than 1%.

Haze is used to characterize the percentage of the transmitted light whose propagation direction deviates a specific angle from the direction of the incident beam. According to the ASTM D1003-13 [40], haze is defined as,

$$H_\lambda = \frac{\tau_{dif,\lambda}}{\tau_{tot,\lambda}} = \frac{\tau_{dif,\lambda}}{\tau_{dif,\lambda} + \tau_{dir,\lambda}} \quad (4)$$

where $\tau_{dif,\lambda}$ refers to the light scattered more than 2.5° off from the incident light [40], and $\tau_{dir,\lambda}$ is the transmitted light within the angle of 2.5°. The diffuse transmittance can be measured by replacing the diffuse reflector at the outlet of the integrating sphere with a light trap to prevent the direct transmittance from influencing the measurement signal. Since the VO_2 nanoparticle size (50 to 80 nm) is much smaller than the wavelength of the visible light (400~ 800 nm), the scattering of the light passing through the PMMA-VO_2 films can be described by Rayleigh scattering [41]. Therefore, it is seen that the haze value decreases as the wavelength increase in Fig. 3(b). The averaged haze value in the visible range is calculated as,

$$H = \frac{\int_{380\ nm}^{780\ nm} H_\lambda I_{lum,\lambda} d\lambda}{\int_{380\ nm}^{780\ nm} I_{lum,\lambda} d\lambda} \tag{5}$$

where H_λ is the measured haze value at wavelength λ. According to Eq. (5), the averaged haze in the luminous range is ~ 11%, as shown in Fig. 3(b). Note that the haze of the developed film could be lowered by reducing the size of the VO_2 nanoparticles [41]. In short, we have fabricated a large-size PMMA-VO_2 film with high luminous transmittance (~ 50%), large solar modulation ability (~ 17.1%), and relatively low haze visibly (~ 11%).

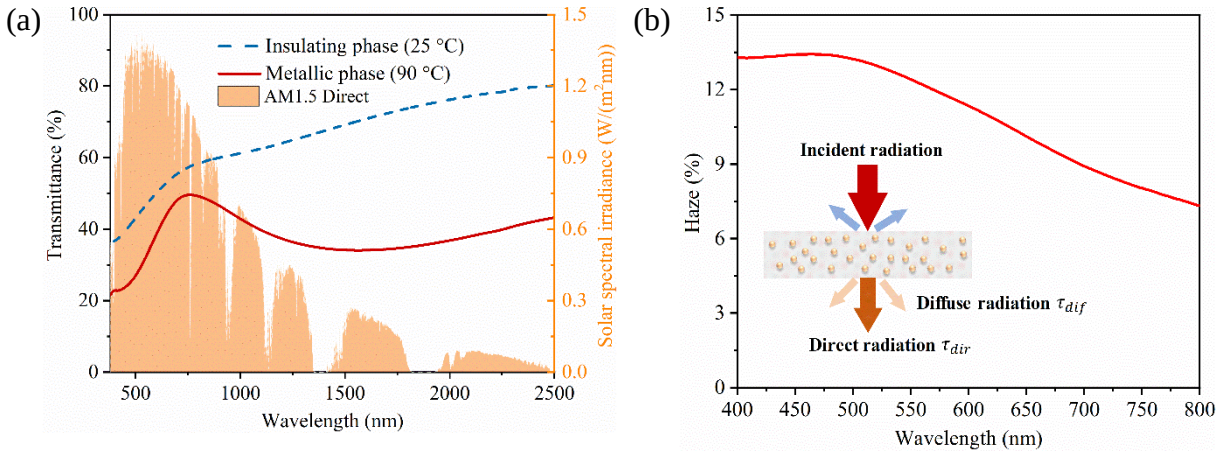

Figure 3. The optical performance of the PMMA-VO_2 film. (a) Spectral transmittance of the PMMA-VO_2 film in the solar spectrum, where the luminous transmittance is ~ 50% and the solar modulation ability is ~ 17.1%. (b) The spectral haze of the PMMA-VO_2 film in the visible range with wavelengths of 400 ~ 800 nm, the averaged haze is ~ 11%.

3.3 Durability of PMMA-VO_2 film

Oxygen and moisture in the ambient air could diffuse into the polymer matrix and oxidize the phase-switchable VO_2 to non-switchable V_2O_5, resulting in the loss of solar modulation ability. It is thus desirable to reduce the diffusion capacity of gas molecules in the polymer matrix. The previous studies have shown that the thermal stability [37], surface hardness, and chemical resistance [42] of the polymer matrix could be improved significantly using entangled and cross-linked molecular chains, which is also directly related to a smaller gas diffusion coefficient. In practice, the natural oxidation of VO_2 is a long process, and the obvious variation of the thermochromic property in the ambient conditions may only be observed after a few months [12]. Thus, accelerated environmental tests were performed to evaluate the durability of VO_2 nanoparticles [43, 44]. The tests were conducted at a temperature of 60 ºC, and the relative humidity ~ 95%, similar to the testing conditions reported in the previous studies [8, 18].

Systematic measurements of spectral transmittance at both low temperature (25 ºC, insulating phase) and high temperature (90 °C, metallic phase) were recorded as a function of time to determine the variation of the thermochromic performance. Each measurement was then repeated at least three times to ensure the testing reliability. To investigate the influence of crosslinking and entanglement on the durability of the PMMA-VO_2 film, the cross-linked and non-crossed-linked PMMA-VO_2 film with two different molecular weights were measured. It is seen that the cross-linked PMMA film with molecular weight ~ 950,000 exhibits no noticeable change in optical transmittance after ~ 200 hours, as shown in Fig. 4 (a). The thermochromic properties of cross-linked PMMA-VO_2 film with molecular weight ~ 950,000 begin to deteriorate after ~ 450 hours exposure while still maintaining more than 60% of its solar modulation ability (~ 10%). After about ~ 900 hours, the solar modulation ability decreased from ~ 17.1% to ~ 4.0%, indicating that a large part of the VO_2 nanoparticles was oxidized. For comparison, the durability performances of the non-cross-linked PMMA with molecular weights ~ 15,000 (Fig. 4(b)) and ~ 950,000 (Fig. 4(c)) were also tested under the same accelerated testing conditions (60 ºC, humidity > 95%). Fig. 4(d) gives the variation of solar modulation abilities of the above three PMMA-VO_2 films as a function of time. It is seen that the decreasing rate of the non-cross-linked film with molecular weight ~ 15,000 is much faster than that of the non-cross-linked PMMA with molecular weight ~ 950,000, which is close to decreasing rate of the uncoated VO_2 in the matrix of resin[16]. The thermochromic performance of the VO_2 in the non-cross-linked PMMA with molecular weights ~ 15,000 disappears after ~ 200 hours. Furthermore, it is found that the lifetime of the cross-linked 950,000 PMMA was approximately 350 hours longer than of non-cross-linked 950,000 PMMA at ~ 600 hours. This indicates that the entangled and crosslinked polymer matrix can substantially improve the lifetime of VO_2 nanoparticles. Fig. 4(d) shows that the lifetime of the PMMA-VO_2

film developed in this work is better than the previously reported values for VO_2 nanoparticles coated by SiO_2 (~ 72 hours) [8], $Al(OH)_3$ (~ 120 hours) [8], and VO_2 thin film protected by Al_2O_3 (~ 100 hours) [14], and is comparable to the performances of VO_2 nanoparticles coated by Al_2O_3 (> 480 hours) [16] and VO_2 thin film protected by SiN_x (~ 600 hours) [18]. Clearly we have demonstrated here an alternative pathway to effectively improve the lifetime of the VO_2 nanoparticles, avoiding the emergence of cracks induced by the periodic insulator-to-metal phase change found in the core-shell structures.

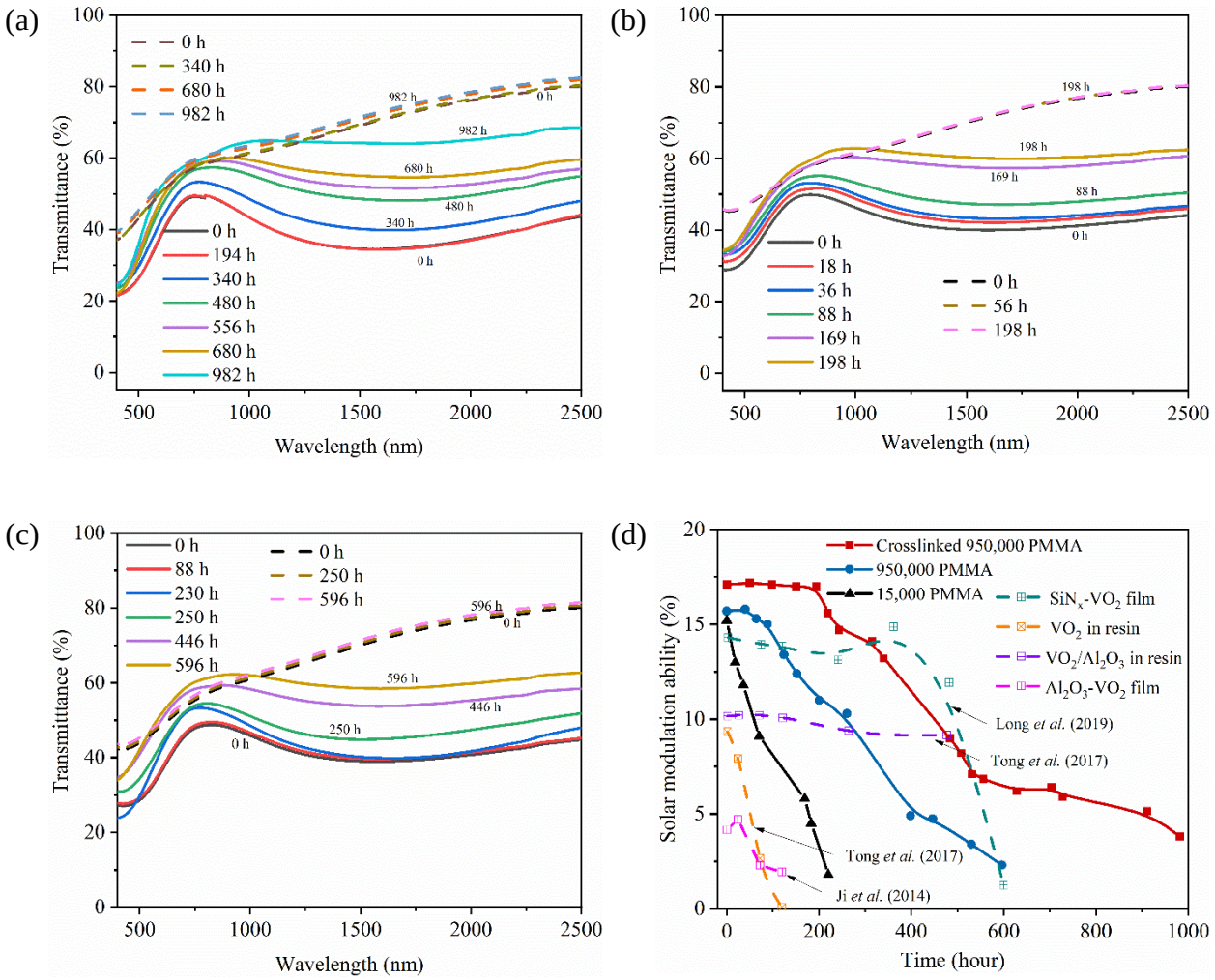

Figure 4. Durability performance of the PMMA-VO_2 films. (a) Variation of the spectral optical transmittance of VO_2 nanoparticles embedded in cross-linked 950,000 PMMA matrix as a function

of aging time. (b) Variation of the spectral optical transmittance of VO_2 nanoparticles embedded in the non-cross-linked 150,000 PMMA matrix as a function of aging time. (c) Variation of the spectral optical transmittance of VO_2 nanoparticles embedded in the non-cross-linked 950,000 PMMA matrix as a function of aging time. (d) Comparison of the solar modulation ability of the VO_2 nanoparticles embedded in non-cross-linked 150,000 PMMA, non-cross-linked 950,000 PMMA, cross-linked 950,000 PMMA matrixes, and previous studies [14, 16, 18]. The low and high temperatures for the optical measurements are 25 ºC (insulating phase) and 90 ºC (metallic phase), respectively. The aging tests were performed in the accelerated aging chamber with a temperature at 60 ºC, and the relative humidity is ~ 95%.

Fatigue tests are used to determine the numbers of cycles (fatigue life) that a material or structure can withstand under cyclic loadings. The emergence of cracks in VO_2-based films or complete fractures may occur due to the lattice transformation of VO_2 during many cycles of phase transitions from the insulating to the metallic state. Therefore, the fatigue test is performed to study the stability of the developed PMMA-VO_2 thermochromic film. The design of the fatigue test can be seen in Fig. 5(a). The PMMA-VO_2 sample coated with a ~ 100 nm thick bottom silver layer was placed on a programmable stage with a temperature control unit (LINKAM MDS600), where the ramping rate was set at (10 °C/min) and an extra 45 seconds delay was assigned to stabilize the temperature of the film at both 25 °C and 90 °C. Meanwhile, the film was constantly exposed to a 633 nm focused laser beam from the helium-neon (HeNe) laser (SIEMENS). The intensity of the transmitted light (μW) was then recorded by the detectors at both low temperature (25 ºC, insulating phase) and high temperature (90 °C, metallic phase) to complete a cycle. Fig. 5(b) shows no noticeable change in transmitted laser intensity in both the metallic and insulator phase after 3000 continuous cycles, indicating that the solar modulation ability of the cross-linked PMMA-

VO_2 remained constant. To ensure the reliability of the test, the measurements were repeated at another two sample locations during each cycle and the results in Fig. 5(b) are the arithmetic average of the three tested points. Note that since incident light traveled across the film twice, the difference between the metallic phase (25 ºC) and the insulator phase (90 ºC) in Fig. 5(b) is approximately twice larger than that of Fig. 3(a).

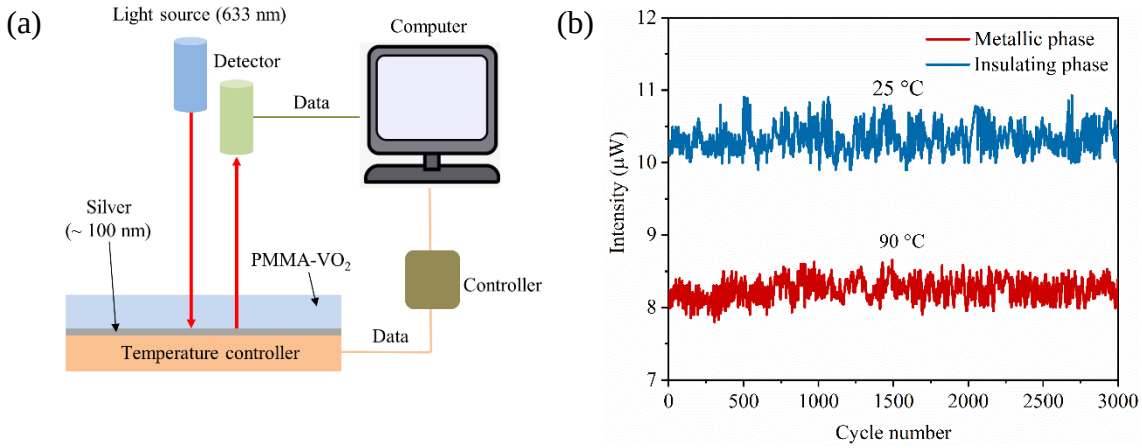

Figure 5. Fatigue test and performance of the PMMA-VO_2 film. (a) Schematic of the setup for fatigue measurements. The temperature of the insulating phase and metallic phase VO_2 were set as 25 °C and 90 ºC, respectively. (b) Variation of the transmittance of the durability enhanced PMMA-VO_2 film as a function of cycle number.

3.4 Thermal comfort and energy saving of PMMA-VO_2 film in different regions

To evaluate the energy saving performance of a PMMA-VO_2 film in different climates and regions, a heat transfer model was developed. Figure 6(a) depicts the heat and solar radiation transfer across a window pane, where the PMMA-VO_2 film with a thickness of ~ 4 μm is employed. The spectral transmittance of the PMMA-VO_2 film in both the insulating phase and the metallic phase was shown in Fig. 3(a). Since the thickness of the window is much smaller than its width

and length, the heat transfer in the *z*-direction can be treated as one-dimensional. Thus, the heat transfer in the z-direction can be described as,

$$k_{gla}\frac{d^2T(z)}{dz^2}+\nabla q(z)=0 \tag{6}$$

where k_{gla} is the thermal conductivity of the float glass, $T(z)$ is the temperature at position *z*, $q(z)$ is the local heat source carried by the solar irradiation, which can be written as

$$q(z)=\tau_{sol}I_o e^{-\beta_{gla}z} \tag{7}$$

where I_o is the incident solar energy, τ_{sol} is the solar transmittance of the PMMA-VO_2 film, and $\beta_{gla}$is the extinction coefficient of the float glass. Compared with the thickness of float glass (3 mm), the thickness of the PMMA-VO_2 (~ 4 μm) film can be ignored. Thus, the boundary conditions at $z=0$ and $z=L_{gla}$ are as follows:

$$q(z=0)=h_o(T_a-T_{z=0})+\sigma\varepsilon_o(T_a^4-T_{z=0}^4)+Q_{abs} \tag{8}$$

$$q\left(z=L_{gla}\right)=h_i\left(T_{z=L_{gla}}-T_r\right)+\sigma\varepsilon_i\left(T_{z=L_{gla}}^4-T_r^4\right) \tag{9}$$

where T_a and T_r are the external ambient temperature and the internal room temperature, respectively, h_e, h_i and $\varepsilon_e, \varepsilon_i$ are the external and internal convective heat transfer coefficients and average external and internal surface emissivities, $\sigma=5.67\times10^{-8}$ (Wm)/K^4 is the Stefan-Boltzmann's constant, $Q_{abs}=\alpha_{sol}I_o$, is the absorbed solar irradiation by the PMMA-VO_2 film, and α_{sol} is the absorbance of the PMMA-VO_2 film. Here, Eq. (6) was solved by the finite volume method [45]. The thermal conductivity and average surface emissivity of the float glass are assumed to be $k_g=0.96$ W/(mK) and $\varepsilon_o\approx0.84$ according to reference [46]. The surface emissivity of the PMMA-VO_2 film is $\varepsilon_o\approx0.9$. From Fig. 3(a), the solar transmittances (τ_{sol}) of

the PMMA-VO_2 film in the insulating phase and metallic phase are 0.57 are 0.40, respectinvely. The reflectances (r_{sol}) of the PMMA-VO_2 in both the insulating and metallic phases were measured as 0.05. Thus, the absorbance can be calculated by $\alpha_{sol} = 1 - \tau_{sol} - r_{sol}$. The inside and external convective heat transfer coefficients can be evaluated by $h_i = 3.6\ \mathrm{W/(m^2K)}$ and $h_o = (10 + 4.1v)\ \mathrm{W/(m^2K)}$, where v (m/s) is the wind speed [46]. The weather conditions including ambient temperature (T_o), window speed (v) and solar irradiation density (I_o) are acquired from the NSRDB Data Viewer [47].

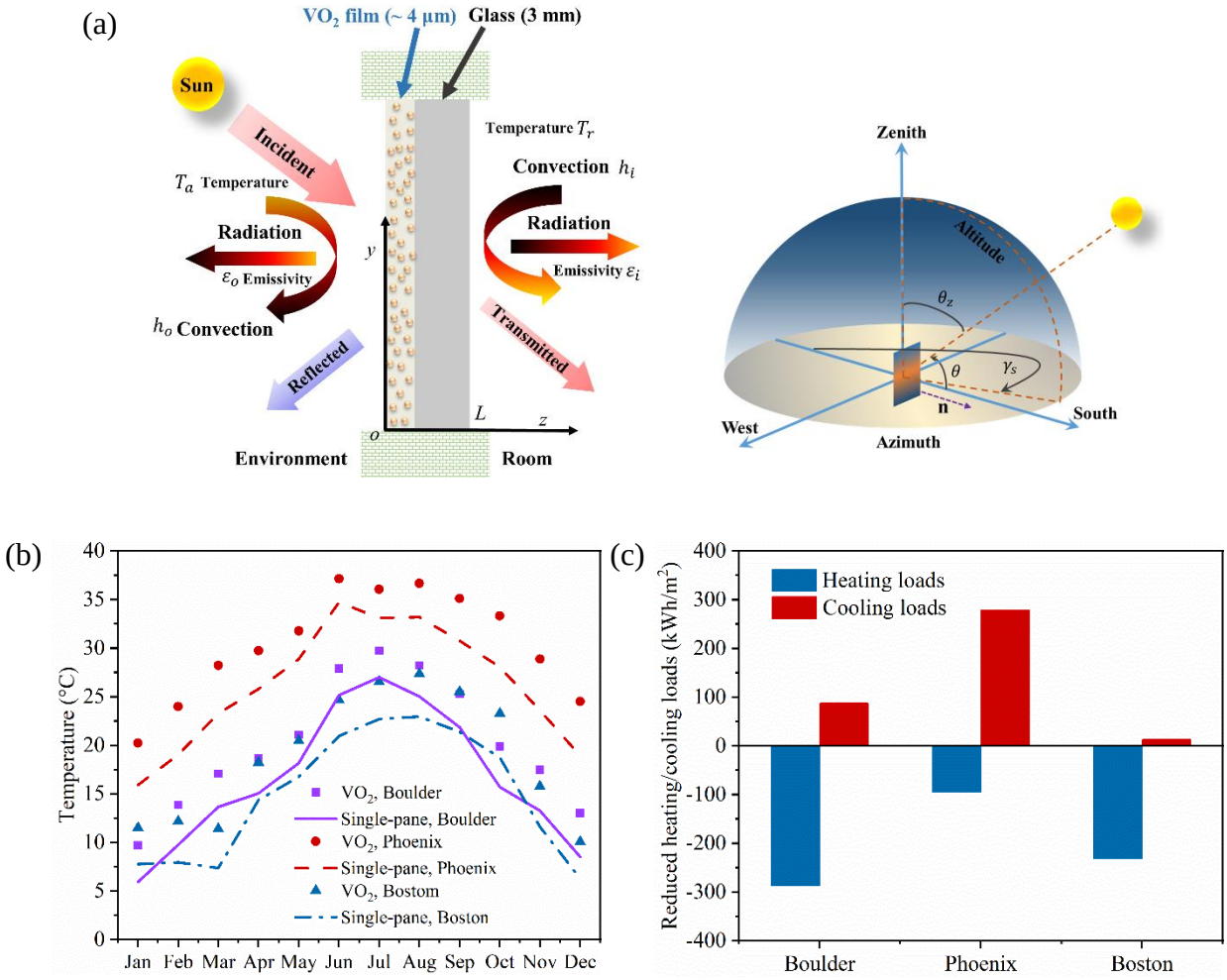

Figure 6. Thermal comfort and energy savings of the PMMA-VO_2 film in selected cities: Boulder (CO), Phoenix (AZ), and Boston (MA). (a) Schematic of heat and radiation energy transfer across

a south-facing single-pane window covered by the PMAA-VO_2 film. (b) Comparison of reduced annual heating/cooling loads of a south-facing window. (c) Influence of PMMA-VO_2 film on the inside surface temperature of a glass window.

The inside surface temperatures of the single-pane window with and without VO_2 film are compared in Fig. 6(b). After employing the PMMA-VO_2 film, the inside surface temperature of the single-pane window is ~ 5 °C higher than that of the single-pane window without a film, indicating that the PMMA-VO_2 film can reduce the temperature difference between the occupants and the innermost surface of windows, which indeed improves the thermal comfort and condensation resistance of the single-pane window in cold climates significantly [48]. Since the solar transmittance of the PMMA-VO_2 film (0.57 ~ 0.4, Fig. 3(a)) is smaller than the single-pane window (~ 90%), applying the PMMA-VO_2 film increase the heating loads in cold climates and reduce the cooling loads in hot climates. Figure 6 (c) compares the reduced annual heating/cooling loads of a south-facing window in different regions. In this Figure, the positive/negative sign represents the reduced/increased energy. For simplicity, it is assumed that the transmitted solar energy decreases (increases) the heating (cooling) loads when the external ambient temperature is higher (lower) than the internal room temperature (21 ºC). Note that the transmitted solar energy includes both the directly transmitted solar irradiation and the absorbed solar energy by window pane and subsequently transferred towards the indoor room environment through heat conduction. Clearly, the cooling demands in the hot areas (e.g., Phoenix) are significantly reduced. However, in the cold areas (e.g., Boston), the increased heating loads in winter are much higher than the reduced cooling loads in summer, indicating that the PMMA-VO_2 film could increase the annual energy cost.

IV. Conclusions

In summary, a thermochromic film based on vanadium dioxide (VO_2) nanoparticles and poly (methyl methacrylate) (PMMA) matrix was proposed and fabricated using the blade coating method. The area and thickness of the fabricated film are 600 mm × 300 mm (length × width) and ~ 4 μm, respectively. It is shown that the PMMA-VO_2 film has a luminous transmittance of ~ 50%, solar modulation ability of ~ 17.1%, and haze of ~ 11%. The solar modulation ability of the PMMA-VO_2 film is higher than that of most previous studies which are usually smaller than 10%. The lifetime of the VO_2 nanoparticles is greatly improved by the cross-linked polymer matrix with high molecular weight. The durability tests were performed in the accelerated aging chamber whose environmental temperature is 60 °C, and humidity is ~ 95%. It was shown that the lifetime of the VO_2 nanoparticles embedded in the cross-linked PMMA matrix with molecular weight ~ 950,000 is ~ 900 hours, which is much longer than that (~ 200 hours) of the VO_2 in the non-cross-linked PMMA matrix with low molecular weight (~ 15,000). The lifetime of the VO_2 nanoparticles in the highly entangled and cross-linked polymer matrix is close to or longer than the lifetime of thermochromic films made of VO_2 protected by environmental stable materials (e.g., aluminum oxide and SiN_x), indicating that cross-linked the polymer chains with high molecular weight could improve the durability of VO_2 remarkably. It was shown that there is no decay of the solar modulation ability after ~ 3000 cycles of fatigue test. The analysis also shows that the PMMA-VO_2 film could greatly reduce the cooling demands in hot climates and improve the thermal comfort in cold climates.

Acknowledgments

X. Zhao and S. Mofid acknowledge the help of Dr. L. Shen., Dr. Y. Zai and Mr. A. Aili on the synthesis of VO_2 nanoparticles and the fabrication of PMMA-VO_2 films, Mr. H. Zhao. and Prof.

G. Cao on the XRD measurements, Mr. D. Alchenberger and Mr. M. Cart from JILA Keck lab on the SEM and optical characterization and Mrs. B. Cunningham for schematics and illustrations. The involvement of researchers from Norway has been supported by the Research Council of Norway through the SINTEF and NTNU research project" High-Performance Nano Insulation Materials" (Hi-Per NIM, project no. 250159) within the NANO2021 program. Furthermore, the Research Council of Norway is acknowledged for the support to the" Norwegian Micro- and Nano-Fabrication Facility" (NorFab, project no. 245963/F50).

Author Contributions

R.Y., X.Y. and B.P.J. designed the research. S.A.M. and X.Y. conceived the experiments, characterization, and modeling. X.Z., S.A.M., T.G., G.T., B.P.J., X.Y, and R.Y. wrote the manuscript. All authors participated in the discussion of the research.

Declaration of Interests

The authors declare no conflict of interest.

References

[1] K. Ismail, J. Henríquez, Thermally effective windows with moving phase change material curtains, Applied Thermal Engineering, 21 (2001) 1909-1923.
[2] R.C. Temps, K. Coulson, Solar radiation incident upon slopes of different orientations, Solar Energy, 19 (1977) 179-184.
[3] Y. Wang, E.L. Runnerstrom, D.J. Milliron, Switchable materials for smart windows, Annual Review of Chemical and Biomolecular Engineering, 7 (2016) 283-304.
[4] H.N. Kim, S. Yang, Responsive Smart Windows from Nanoparticle-Polymer Composites, Advanced Functional Materials, (2019) 1902597.
[5] Y. Ke, C. Zhou, Y. Zhou, S. Wang, S.H. Chan, Y. Long, Emerging thermal- responsive materials and integrated techniques targeting the energy- efficient smart window application, Advanced Functional Materials, 28 (2018) 1800113.
[6] Y. Cui, Y. Ke, C. Liu, Z. Chen, N. Wang, L. Zhang, Y. Zhou, S. Wang, Y. Gao, Y. Long, Thermochromic VO_2 for energy-efficient smart windows, Joule, (2018).
[7] Z. Chen, Y. Gao, L. Kang, C. Cao, S. Chen, H. Luo, Fine crystalline VO_2 nanoparticles: synthesis, abnormal phase transition temperatures and excellent optical properties of a derived VO_2 nanocomposite foil, Journal of Materials Chemistry A, 2 (2014) 2718-2727.

[8] Y. Chen, X. Zeng, J. Zhu, R. Li, H. Yao, X. Cao, S. Ji, P. Jin, High performance and enhanced durability of thermochromic films using VO_2@ ZnO core–shell nanoparticles, ACS Applied Materials & Interfaces, 9 (2017) 27784-27791.
[9] S.-Y. Li, G.A. Niklasson, C.-G. Granqvist, Nanothermochromics: calculations for VO_2 nanoparticles in dielectric hosts show much improved luminous transmittance and solar energy transmittance modulation, Journal of Applied Physics, 108 (2010) 063525.
[10] Y. Gao, S. Wang, H. Luo, L. Dai, C. Cao, Y. Liu, Z. Chen, M. Kanehira, Enhanced chemical stability of VO_2 nanoparticles by the formation of SiO_2/VO_2 core/shell structures and the application to transparent and flexible VO_2-based composite foils with excellent thermochromic properties for solar heat control, Energy & Environmental Science, 5 (2012) 6104-6110.
[11] Y. Li, S. Ji, Y. Gao, H. Luo, P. Jin, Modification of Mott phase transition characteristics in VO_2@ TiO_2 core/shell nanostructures by misfit-strained heteroepitaxy, ACS Applied Materials & Interfaces, 5 (2013) 6603-6614.
[12] L. Zhao, L. Miao, C. Liu, C. Li, T. Asaka, Y. Kang, Y. Iwamoto, S. Tanemura, H. Gu, H. Su, Solution-processed VO_2-SiO_2 composite films with simultaneously enhanced luminous transmittance,solar modulation ability and anti-oxidation property, Scientific reports, 4 (2014) 7000.
[13] R. Lindström, V. Maurice, S. Zanna, L. Klein, H. Groult, L. Perrigaud, C. Cohen, P. Marcus, Thin films of vanadium oxide grown on vanadium metal: oxidation conditions to produce V_2O_5 films for Li-intercalation applications and characterisation by XPS, AFM, RBS/NRA, Surface and Interface Analysis, 38 (2006) 6-18.
[14] Y.-X. Ji, S.-Y. Li, G.A. Niklasson, C.G. Granqvist, Durability of thermochromic VO_2 thin films under heating and humidity: effect of Al oxide top coatings, Thin Solid Films, 562 (2014) 568-573.
[15] T. Chang, X. Cao, L.R. Dedon, S. Long, A. Huang, Z. Shao, N. Li, H. Luo, P. Jin, Optical design and stability study for ultrahigh-performance and long-lived vanadium dioxide-based thermochromic coatings, Nano Energy, 44 (2018) 256-264.
[16] K. Tong, R. Li, J. Zhu, H. Yao, H. Zhou, X. Zeng, S. Ji, P. Jin, Preparation of VO_2/Al-O core-shell structure with enhanced weathering resistance for smart window, Ceramics International, 43 (2017) 4055-4061.
[17] Y. Li, S. Ji, Y. Gao, H. Luo, M. Kanehira, Core-shell VO_2@TiO_2 nanorods that combine thermochromic and photocatalytic properties for application as energy-saving smart coatings, Scientific Reports, 3 (2013) 1370.
[18] S. Long, X. Cao, N. Li, Y. Xin, G. Sun, T. Chang, S. Bao, P. Jin, Application-oriented VO_2 thermochromic coatings with composite structures: optimized optical performance and robust fatigue properties, Solar Energy Materials and Solar Cells, 189 (2019) 138-148.
[19] A. Huang, Y. Zhou, Y. Li, S. Ji, H. Luo, P. Jin, Preparation of $V_xW_{1-x}O_2$(M)@SiO_2 ultrathin nanostructures with high optical performance and optimization for smart windows by etching, Journal of Materials Chemistry A, 1 (2013) 12545-12552.
[20] Ö. Pekcan, Ş. Uğur, Molecular weight effect on polymer dissolution: a steady state fluorescence study, Polymer, 43 (2002) 1937-1941.
[21] L.H. Sperling, Introduction to physical polymer science, John Wiley & Sons, 2005.
[22] K. Balani, V. Verma, A. Agarwal, R. Narayan, Physical, Thermal, and Mechanical Properties of Polymers, in, John Wiley & Sons, Inc, Hoboken, NJ, United States, 2014.
[23] L. Tan, F. Yang, M.R. Kim, P. Li, D.T. Gangadharan, J.l. Margot, R. Izquierdo, M. Chaker, D. Ma, Enhanced long-term and thermal stability of polymer solar cells in air at high humidity with the formation of unusual quantum dot networks, ACS Applied Materials & Interfaces, 9 (2017) 26257-26267.
[24] S.C. George, S. Thomas, Transport phenomena through polymeric systems, Progress in Polymer Science, 26 (2001) 985-1017.
[25] A. Berens, H. Hopfenberg, Diffusion of organic vapors at low concentrations in glassy PVC, polystyrene, and PMMA, Journal of Membrane Science, 10 (1982) 283-303.
[26] M. Klinger, L.P. Tolbod, K.V. Gothelf, P.R. Ogilby, Effect of polymer cross-links on oxygen diffusion in glassy PMMA films, ACS Applied Materials & Interfaces, 1 (2009) 661-667.

[27] M. Li, S. Magdassi, Y. Gao, Y. Long, Hydrothermal synthesis of VO_2 polymorphs: advantages, challenges and prospects for the application of energy efficient smart windows, Small, 13 (2017) 1701147.
[28] W. Li, S. Ji, Y. Li, A. Huang, H. Luo, P. Jin, Synthesis of VO_2 nanoparticles by a hydrothermal-assisted homogeneous precipitation approach for thermochromic applications, RSC Advances, 4 (2014) 13026-13033.
[29] R. Li, S. Ji, Y. Li, Y. Gao, H. Luo, P. Jin, Synthesis and characterization of plate-like VO_2 (M)@SiO_2 nanoparticles and their application to smart window, Materials Letters, 110 (2013) 241-244.
[30] U. Ali, K.J.B.A. Karim, N.A. Buang, A review of the properties and applications of poly (methyl methacrylate)(PMMA), Polymer Reviews, 55 (2015) 678-705.
[31] D.J. Carbaugh, J.T. Wright, R. Parthiban, F. Rahman, Photolithography with polymethyl methacrylate (PMMA), Semiconductor Science and Technology, 31 (2015) 025010.
[32] C. Wochnowski, M.S. Eldin, S. Metev, UV-laser-assisted degradation of poly (methyl methacrylate), Polymer Degradation and Stability, 89 (2005) 252-264.
[33] H. Albeladi, A. Al-Romaizan, M. Hussein, Role of cross-linking process on the performance of PMMA, Int. J. Biosens. Bioelectron, 3 (2017) 279-284.
[34] S. Eve, J. Mohr, Study of the surface modification of the PMMA by UV-radiation, Procedia Engineering, 1 (2009) 237-240.
[35] M.M. Qazilbash, M. Brehm, B.-G. Chae, P.-C. Ho, G.O. Andreev, B.-J. Kim, S.J. Yun, A. Balatsky, M. Maple, F. Keilmann, Mott transition in VO_2 revealed by infrared spectroscopy and nano-imaging, Science, 318 (2007) 1750-1753.
[36] Y. Kim, S. Yu, J. Park, D. Yoon, A.M. Dayaghi, K.J. Kim, J.S. Ahn, J. Son, High-throughput roll-to-roll fabrication of flexible thermochromic coatings for smart windows with VO_2 nanoparticles, Journal of Materials Chemistry C, 6 (2018) 3451-3458.
[37] M.A. Hussein, R.M. El-Shishtawy, B.M. Abu-Zied, A.M. Asiri, The impact of cross-linking degree on the thermal and texture behavior of poly (methyl methacrylate), Journal of Thermal Analysis and Calorimetry, 124 (2016) 709-717.
[38] G. Wyszecki, W.S. Stiles, Color science, Wiley New York, 1982.
[39] C. Riordan, R. Hulstron, What is an air mass 1.5 spectrum?(Solar cell performance calculations), in: IEEE Conference on Photovoltaic Specialists, IEEE, 1990, pp. 1085-1088.
[40] ASTM D1003-13-Standard test method for haze and luminous transmittance of transparent, ASTM International West Conshohocken, 2013.
[41] C.F. Bohren, D.R. Huffman, Absorption and scattering of light by small particles, John Wiley & Sons, 2008.
[42] B.J. Park, M.S. Kim, H.J. Choi, Fabrication and magnetorheological property of core/shell structured magnetic composite particle encapsulated with cross-linked poly (methyl methacrylate), Materials Letters, 63 (2009) 2178-2180.
[43] B.P. Jelle, Accelerated climate ageing of building materials, components and structures in the laboratory, Journal of Materials Science, 47 (2012) 6475-6496.
[44] B.P. Jelle, E. Sveipe, E. Wegger, A. Gustavsen, S. Grynning, J.V. Thue, B. Time, K.R. Lisø, Robustness classification of materials, assemblies and buildings, Journal of Building Physics, 37 (2014) 213-245.
[45] R. Eymard, T. Gallouët, R. Herbin, Finite volume methods, Handbook of Numerical Analysis, 7 (2000) 713-1018.
[46] B.P. Jelle, Solar radiation glazing factors for window panes, glass structures and electrochromic windows in buildings-Measurement and calculation, Solar Energy Materials and Solar Cells, 116 (2013) 291-323.
[47] https://maps.nrel.gov/nsrdb-viewer/.
[48] P. Lyons, D. Arasteh, C. Huizenga, Window performance for human thermal comfort, Transactions-American Society of Heating Refrigerating and Air Conditioning Engineers, 106 (2000) 594-604.

Declaration of competing Interest

☒ The authors declare that they have no known competing financial interests or personal relationships that could have appeared to influence the work reported in this paper.

☐The authors declare the following financial interests/personal relationships which may be considered as potential competing interests:

Credit Author Statement

R.Y., X.Y. and B.P.J. designed the research. S.A.M. and X.Y. conceived the experiments, characterization, and modeling. X.Z., S.A.M., T.G., G.T., B.P.J., X.Y, and R.Y. wrote the manuscript. All authors participated in the discussion of the research.